INTERNAL BALLISTICS OF SOLID FUEL RAMJETS

Lowell David Boaz

NAVAL POSTGRADUATE SCHOOL
Monterey, California

THESIS

INTERNAL BALLISTICS
OF
SOLID FUEL RAMJETS

by

Lowell David Boaz

Thesis Advisor: D. W. Netzer

March 1973

Internal Ballistics of Solid Fuel Ramjets

by

Lowell David Boaz
Lieutenant, United States Navy
B.S., United States Naval Academy, 1967

Submitted in partial fulfillment of the
requirements for the degree of

MASTER OF SCIENCE IN AERONAUTICAL ENGINEERING

from the

NAVAL POSTGRADUATE SCHOOL
March 1973

ABSTRACT

An experimental investigation of the internal ballistics of solid fuel ramjets was conducted in order to determine the regression rate of the fuel as a function of chamber pressure, inlet air temperature, and air flux rate, and to model the flow in solid fuel ramjets which use sudden expansion flameholders at the inlet. In addition, flame stabilization limits were investigated. A computer solution for the non-reacting flow field gave results in good agreement with experiments.

Solid fuel ramjets have an average regression rate of the fuel that closely follows the theoretical expression derived for kinetically controlled hybrid rocket combustion. The inlet step-height-to-motor-diameter ratio is the dominant parameter in determining flame stability limits. However, inlet velocity is also an important parameter.

TABLE OF CONTENTS

LIST OF TABLES

LIST OF FIGURES

ACKNOWLEGEMENTS

The author wishes to express his appreciation to Associate Professor David W. Netzer of the Department of Aeronautics for his guidance, encouragement, and assistance throughout the project.

Appreciation also goes to Edward Michelson, Patrick J. Hickey, Jr. and Cecil R. Gordon who with the remainder of the technical staff of the Aeronautics Department furnished timely and efficient technical assistance.

This work was sponsored by the Naval Weapons Center, China Lake, California under Work Request 2-3044.

I. INTRODUCTION

The solid fuel ramjet can be classified as a special case of the hybrid rocket. That is, the fuel is solid and the oxidizer is gaseous (air). The solid fuel ramjet provides many of the advantages of solid fuel rockets without the weight penalty of carrying its own oxidizer. Ease of handling, storability, weight savings, and possibly greatly increased tactical ranges are among its advantages.

A research project is currently being conducted at the Naval Postgraduate School to model the internal ballistics of solid fuel ramjets. Such a model would provide the design engineer with a working tool that would permit performance parameters and operating characteristics to be predicted. The overall goal of the research project is to develop a model that can predict the regression rate of the fuel as a function of operating and configuration variables. Very little experimental data currently exist that can be used to determine the adequacy of a model, thus the model must be developed in steps verifying each step with experimental data. Non-burning tests to determine flow patterns, non-burning tests with wall blowing to determine the effect of wall mass addition on the flow characteristics, and hot firing tests with various inlet geometries are required. This thesis initiates the overall research project objectives.

Information is provided from several areas of study that are pertinent to the internal ballistics of solid fuel ramjets. Specific areas are flow and heat transfer in ducts with a backward facing step, flame stabilization in high speed flows, hybrid rocket combustion, and thermal decomposition of polymers.

Abbott and Kline [Ref. 1] investigated the turbulent flow over backward facing steps using water flow through a two-dimensional channel. It was found that the recirculation zone consisted of a complex pattern involving three distinct regions. Immediately downstream of the step face there is a three-dimensional zone "characterized by one or more vortexes rotating about an axis normal to the vertical wall." This zone is followed by an almost two-dimensional zone of recirculating flow. The area at the flow reattachment point is characterized by a fluctuating three-dimensional flow. It was also found that the location of the reattachment point remained fixed as Reynolds number and/or inlet turbulence intensity varied, and that increasing the step height moved the reattachment point further downstream from the step face.

Krall and Sparrow [Ref. 2] using water flow through an orifice in an electrically heated circular tube found that local heat transfer coefficients in the separated, reattached, and redevelopment regions are several times larger than those for fully developed turbulent pipe flow. They found that

the maximum heat transfer coefficient occurred in the vicinity of the point of flow reattachment.

At low Reynolds numbers based on downstream pipe diameter (10,000 to 50,000) the heat transfer near the reattachment point varied rapidly with Reynolds number. However, at higher Reynolds numbers (70,000 to 130,000) only a weak dependence was noted. They also found that for weaker separations (small step heights, h) the reattachment point was well defined but for strong separations (large step heights) the reattachment point was spread out. This transition from a single well-defined reattachment point to the "spread-out" configuration occurred between h/D=0.16 and h/D=0.25, where D is the downstream pipe diameter. The reattachment point was located between 1.25 and 2.5 pipe diameters downstream of the initial separation. Increased step height moved the reattachment point slightly downstream. Reynolds number and Prandtl number had no significant effect on the reattachment point location.

The results of Krall and Sparrow are also in general agreement with the results of Abbott and Kline. For small step heights (h/D=.17) the two-dimensional and axisymmetric reattachment points are very nearly equal (X_r/D from 1.0 to 1.25). However, for larger step heights, the reattachment zone spreads out considerably more for the two-dimensional case than for the axisymmetric case.

The ideal hybrid rocket is one in which a gaseous oxidizer flows over a solid fuel. In a hybrid rocket, gas

phase combustion in the form of a diffusion flame takes place in the turbulent boundary layer formed by the oxidizer flow over the solid surface of the fuel. Heat is transported by convection and radiation to the solid surface which causes decomposition of the fuel. The convective heat transport is complicated by the presence of high rates of wall mass addition. Using a heat transfer limited model, regression rates of the fuel are generally proportional to G^n, where G is the total gas flux and n is a constant (typically 0.8).

Experimental data obtained at low chamber pressure and/or high oxidizer mass flux indicate that the regression rate of hybrid grains becomes less dependent on G, but is directly related to the partial pressure of the oxidizer in the gas phase [Refs. 3 and 4]. Reduced reaction rates at lower pressures broaden the flame zone. Schlieren studies have also shown that the flame zone broadens at low chamber pressures and may broaden enough to undergo transition to a turbulent premixed flame [Ref. 6]. When the oxidizer is diluted, the diffusion flame moves further away from the surface, increases in thickness, and the flame temperature drops [Refs. 3 and 5]. In addition, surface kinetics may be rate controlling under these operating conditions [Ref. 7]. When these conditions exist, the heat transfer limited model does not adequately describe the combustion process.

Hybrid rockets operating at high chamber pressures are adequately described by a heat transfer limited model. Muzzy [Ref. 4] has reviewed the modifications that have been made to the heat transfer limited model to account for gas phase and surface kinetic effects. The modified models [Refs. 6 and 7] predict a dependence of the regression rate on pressure as well as mass flow rate. For a system where radiative heat transfer can be neglected, Muzzy has shown that the regression rate equation in the kinetically dominated region of operation can be expressed as:

$$\dot{r} = C\ P^{0.5}\ G^{a}\ X^{b}$$

where C is a constant, P is pressure, G is total mass flux, X is the longitudinal coordinate, a is a constant that varies from 0.3 to 0.4, and b is a constant that varies from -0.1 to -0.2. Another study by Kustov and Rybanin [Ref. 18] has also treated the pressure sensitive regime of operation.

In a solid fuel ramjet the reacting flow has characteristics that are similar to those discussed above. However, two significant differences exist. Solid fuel ramjets would normally operate at lower chamber pressures than hybrid rockets, resulting in significantly greater port velocities. In addition, the oxidizer in this case is air which would correspond to a severely diluted oxidizer in hybrid combustion. These differences require some means of flame stabilization. A series of tests performed at the United Technology Center [Ref. 8] have shown that one means of

sustaining combustion in a solid fuel ramjet is to use a sudden expansion inlet as is used in dump combustors. Similar results were reported by McCarthy [Ref. 9].

In a high velocity gas stream, where the velocities of the flow are at least an order of magnitude greater than the turbulent flame speeds of the combustion mixtures, flame stabilization is required. Bluff body flame stabilization has been used successfully in turbojet and liquid fuel ramjet combustor design in the past. Typical flame stabilizers have been V-gutters and rods, or the dome of a can-type combustor [Refs. 10 and 11]. In addition, dump or sudden expansion combustors have been studied for integral rocket/liquid ramjet designs [Ref. 19].

The recirculation zone behind the bluff body or step causes intense mixing of fresh unburned fuel and air with hot combustion products. The hot combustion products ignite the fuel-air mixture. This stabilized flame can then propagate throughout the combustor. Due to the intense turbulent mixing in the recirculation zone, combustion may in some cases approach that of a well-stirred reactor.

A well-stirred reactor model considers the composition and all of the thermodynamic properties to be uniform throughout the volume. An idealized reactor with instantaneous mixing would have homogeneous fuel, air, and product concentrations, and constant pressure and temperature [Refs. 12 and 13].

Solid fuel ramjet combustors have, depending upon the combustor length and inlet configuration, two separate and distinct combustion zones, each of which appears to be controlled by a different mechanism [Ref. 9] (See Figure 1). In the recirculation zone products and reactants are rapidly mixed, and in the limiting case a well-stirred reactor may be approached. Downstream of the flow reattachment point the boundary layer develops and the combustion may be similar to that in a hybrid rocket in which kinetic effects are dominant (low pressure, high mass flux, severe oxidizer dilution).

Thus, one possible model for solid fuel ramjet combustion would be to treat the recirculation region as a well-stirred reactor and the downstream region as a kinetically dominated hybrid. The larger the grain length-to-diameter ratio, the more dominant the downstream region becomes in determining the average regression rate, and the more one could expect the ramjet to behave as a kinetically controlled hybrid combustor. However, for small L/D ratios and/or large recirculation zones, the combustion in the recirculation region may become important in determination of the average regression rate. In addition, the combustion characteristics in the recirculation region determine the flammability limits for the entire combustor. Thus, the model used in this region requires considerable attention. For very strong recirculation zones, a well-stirred reactor model may be adequate. However, for weaker recirculation

zones, which are desirable from a pressure loss standpoint, kinetic rates may be of the same order or greater than the reactant mixing rates. In this case, a well-stirred reactor model cannot be expected to be applicable and a more detailed consideration of the recirculating flow is necessary. Thus, the work of Gosman, et al. [Ref. 14] and Spalding, et al. [Ref. 15] becomes increasingly important and may provide the basis for modeling the recirculation region in solid fuel ramjet combustors.

It is the purpose of this study to determine the dependence of the regression rate of a solid fuel ramjet on chamber pressure, inlet air temperature, and mass flux of air, and to model the flow in the recirculation region caused by the sudden expansion inlet.

II. METHOD OF INVESTIGATION

Non-burning flow visualization tests were conducted using a plexiglass model with three inlet step configurations. Flow reattachment points of the incoming stream were measured for various step Reynolds number flows.

A Fortran language computer program, Pistep II, developed by Spalding, et al. [Refs. 14 and 15] provided a finite difference solution of the two dimensional Navier-Stokes equations governing heat and mass transfer in recirculating flows. It was used to calculate the flow reattachment point and the flow field for non-burning flows. The results were compared with the flow visualization data and the work of previous investigators. The boundary conditions on the differential equations were altered to simulate blowing at the wall in order to study the effect of mass injection from the wall on the flow field.

Experimental firings were conducted using polymethylmethacrylate grains burning with non-vitiated air to provide regression rate data as a function of inlet air temperature, chamber pressure, and oxidizer flux rate. These tests were made to provide initial data for characterizing ramjet combustion and flame blow-off limits, and to determine if the reacting flow behavior was similar to that obtained analytically and experimentally for non-burning flow.

III. DESCRIPTION OF APPARATUS

A. COLD FLOW VISUALIZATION MODEL

The flow visualization model (Figure 2) consisted of three sections. The first section was a 2½ x 2½ x 5-inch plexiglass block with a three-quarter inch diameter hole bored through the center. It received air from high pressure tanks and supported a perforated disk flow straightener. The step section was made of stainless steel and was ten inches in length to further dampen turbulence and provide fully developed velocity profiles. Three steps were used with inside diameters of 0.246, 0.519, and 0.714 inches respectfully. The third section was a 15½-inch plexiglass tube with an inside diameter of 1.469 inches.

For the lower flow rates a sonic choke with a diameter of 0.081 inches was used to measure flow rates. For higher flow rates, an orifice flow meter with inputs to a Visicorder was used to measure flow rates. The flow reattachment points were measured visually using a scale.

B. HOT FIRING APPARATUS

A schematic of the solid fuel ramjet apparatus showing the overall system is presented in Figure 3.

1. Ramjet Motor

The solid fuel ramjet motor consisted of four main sections: the head end assembly, the step insert section, the grain, and the aft closure section (Figure 4). All of

the metal parts of the motor except for the bolts were made of stainless steel.

The head end assembly was 6¼ inches long and contained the inlets for the air, the oxygen-methane ignition mixture, the nitrogen purge, and the cooling air. Two Champion Z7 spark plugs were used for ignition.

The step insert section was 2-3/4 inches long and held the step in place. Three steps were used during this investigation with inside diameters of 0.25, 0.50, and 0.75 inches. This section also accomodated the forward end of the PMM grain.

Polymethylmethacrylate was chosen as the fuel in this study because it has been widely used for basic research in hybrid rocket combustion and in studies of polymer degradation in the past. It is composed of long chains of a repeating monomer:

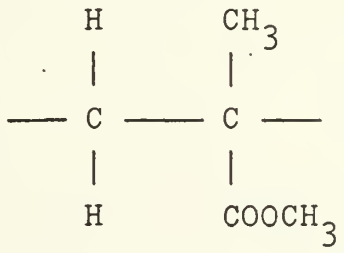

Idealized chemical reaction with complete combustion would involve a stoichiometric reaction with air as follows:

$$C_5H_8O_2 + 6O_2 + 22.56N_2 \rightarrow 4H_2O + 5CO_2 + 22.56N_2$$

The average molecular weight of the products in this case

is 31.3 lbm/lbmole. The gas constant is $\bar{R}/M$ = 49.4 ft-lbf/lbm-°R, and the stoichiometric air fuel ratio is 8.27 lbmair/lbmfuel. The equilibrium ratio of specific heats at a temperature of 3500°R is γ = 1.24. An adiabatic flame temperature calculation for the stoichiometric reaction using a value of $\bar{H}_f^o$ of 92.8 kcal/mole for the heat of formation of PMM at 25 °C [Ref. 5] gives a flame temperature (with no dissociation) of 4265 °R.

The polymethylmethacrylate grains were cut from a slab into 3-3/4 x 3-3/4 x 12 inch blocks. The ends were rounded to an outside diameter of 3-1/2 inches to fit into the step section and the aft closure section, and were sealed with "O" ring seals. The initial inside port diameter of the grains was 1.5 inches. Eight grains were made that were six inches in length, but the majority of the tests were performed using grains that were 12 inches in length.

The aft closure section contained a straight section with a pressure tap and a converging-diverging nozzle. Nine nozzles with various throat areas were used to control the chamber pressure. A Wiancko 0-200 psig pressure transducer was mounted on the forward part of the aft closure section to measure the chamber pressure.

The grains were held in place by four 3/8 inch diameter steel rods between the step section and the aft closure section. Mounting flanges on the head end assembly and the aft closure section were bolted to a large test stand.

2. Ignition System

The ignition system metered oxygen and methane at 800 psig from two high pressure tanks through needle valves into the head end assembly section. Inlet ports on the top and the bottom injected methane, and two inlet ports injected oxygen from either side. Two inches downstream from the oxygen-methane ports were two Champion Z7 spark plugs located 180 degrees apart. A transformer supplied power to a Model T spark coil to energize the spark plugs.

3. Nitrogen Purge and Cooling Air System

The nitrogen purge and cooling air system was connected upstream of the head assembly section. Two high pressure tanks fed nitrogen into the motor at the end of a hot firing for approximately one second to extinguish the combustion flame. Cooling air from a low pressure compressor was then blown through the motor.

4. Air Flow Control

A standard ASME orifice flow meter was used to measure the flow rate of the air into the motor. A manually operated gate valve between the orifice and the motor was used to provide the desired flow rate through the motor. Two pneumatically operated Jamesbury ball valves operating together either vented the air to the atmosphere, or allowed the air to pass through the motor.

5. Data Acquisition System

A Colvin 0-35 psi differential pressure transducer was used to measure the pressure drop across the orifice

flow meter. A Wiancko 0-200 psig pressure transducer was used to measure the pressure upstream of the orifice, and an iron-constantan thermocouple was used to measure the temperature at the orifice. A second iron-constantan thermocouple was used to measure the temperature of the air entering the motor. A Wiancko 0-200 psig pressure transducer measured chamber pressure at the aft closure section of the motor.

The orifice thermocouple output was recorded on a 0-600°F strip chart recorder. All of the other transducer outputs were recorded on a Honeywell Model 2106 Visicorder. A five cycle per second timing signal and an ignition pulse were also recorded on the Visicorder.

6. Air Feed System

A Pennsylvania air compressor provided air at pressures up to 150 psia at a rate of up to 700 scfm. This air was fed into an air reservoir and a Polytherm air heater. The Polytherm air heater was capable of yielding 1.75 pounds per second airflow at 150 psia and 1000°F. The heater burned natural gas, and the air passed through a heat exchanger, thus providing non-vitiated hot air.

A temperature controller directed two mixing valves that produced the required air temperature at 150 psia. A manual gate valve controlled the air flow to the test cell. A valve in the test cell controlled the flow of air to the pipe leading to the orifice flow meter.

Figures 5, 6, 7, and 8 show the test cell and the ramjet apparatus.

IV. EXPERIMENTAL PROCEDURE

A. COLD FLOW TESTS

The cold flow tests were performed at the rocket lab facilities of the Naval Postgraduate School. Visualization was obtained by injecting a mixture of water, alcohol, and food coloring at the base of the step inlet through a small tube with a hypodermic needle. The mixture was broken up into very small droplets by the turbulence in the recirculation zone. In the recirculation zone the droplets on the wall moved towards the step. At the flow reattachment point the droplets on the wall were stationary. Downstream of the reattachment point the droplets on the wall moved away from the step. Using this technique, the flow reattachement point locations for various step Reynolds number flows using three step sizes were measured visually using a scale.

Initial visualization tests were attempted using a tufted model but they proved to be of limited value due to the highly turbulent nature of the flow.

B. HOT FIRING TESTS

All hot firing tests were performed in the jet engine test cell at the Naval Postgraduate School. Hot firing data were obtained from a series of firings at three air flow rates, three chamber pressures, and three inlet temperatures, using three step heights and two grain lengths. The majority of the hot firings were performed with a 12 inch

grain length and an inlet diameter of 0.5 inches. Table I summarizes the nominal test conditions.

TABLE I

NOMINAL TEST CONDITIONS

Chamber Pressure (psia)	50	75	100
Air Flow Rate (lbm/sec)	.15	.25	.40
Inlet Temperature (°F)	70	200	350
Inlet Diameter (in)	.25	.50	.75
Step h/D	.417	.333	.25
Grain Length (in)	12	6	

For the tests in which the Polytherm air heater was used, the temperature controller was set and the temperature would stabilize at the ramjet inlet in one to two hours. This delay was due to the fact that the flow rates to the motor were quite low, at most 0.5 lbm/sec. Once the temperature stabilized at the desired temperature at the inlet to the ramjet, the manual gate valve downstream of the orifice was set to obtain the desired air flow rate.

Chamber pressures were preselected and controlled by varying the nozzle throat area for a given air flow rate. Chamber pressures could normally be attained within ten psi of the desired pressure. Calculated combustion temperatures

varied significantly with air flow rate and step size. Also, at higher chamber pressures the preset flow rate would decrease upon ignition because the higher back pressure would unchoke the air flow control valve.

Ignition normally lasted for four seconds. After three seconds of ignition, the air was directed through the ramjet motor. Ignition was continued into the first second of the run to insure that combustion would be sustained. A series of thirteen tests at high flow rates in which the ignition flame was blown out were used to determine the rate of consumption of the PMM grains during the oxygen-methane ignition. These data were used to correct the initial weight of the fuel used in the regression rate calculation.

Combustion lasted for thirty seconds. At the end of each run the motor was extinguished by simultaneously venting the air to the atmosphere with the Jamesbury ball valves and actuating the nitrogen purge system. Low pressure air was then blown through the motor for cooling. The only section of the motor that heated up significantly was the aft closure section and the nozzle.

V. PISTEP II COMPUTER PROGRAM

Pistep II is a Fortran computer program developed by Gosman, Pun, Runchal, Spalding, and Wolfshtein [Ref. 14]. It provides a finite difference solution of a steady incompressible turbulent flow through a cylindrical pipe with a sudden step enlargement. Equations [Ref. 15] governing the distribution of stream function, ψ, vorticity, ω/r, non-dimensional temperature, T, turbulent kinetic energy, k, and turbulent energy dissipation rate, ε, are cast in elliptic form in cylindrical polar coordinates as follows:

$$a_\phi\left[\frac{\partial}{\partial z}\left(\phi\,\frac{\partial\psi}{\partial r}\right)-\frac{\partial}{\partial r}\left(\phi\,\frac{\partial\psi}{\partial z}\right)\right]-\frac{\partial}{\partial z}\left[b_\phi r\,\frac{\partial(C_\phi\phi)}{\partial z}\right]$$

$$-\frac{\partial}{\partial r}\left[b_\phi r\,\frac{\partial(C_\phi\phi)}{\partial r}\right]+r S_\phi = 0$$

where ϕ represents any one of the variables ψ, ω/r, k, ε, or T. The functions a_ϕ, b_ϕ, C_ϕ, and S_ϕ are presented in Table II.

A two equation turbulence model is employed in the program. The two variables are turbulent kinetic energy, k, and the turbulent energy dissipation rate, ε. The effective viscosity, μ_{eff}, is related to k and ε by

$$\mu_{eff} = C_\mu \rho k^2/\varepsilon$$

A "dissipation length scale", ℓ, can be used in an alternative formulation:

$$\mu_{eff} = C_\mu k^{1/2} \rho \ell$$

Equating the two equations for the effective viscosity gives:

$$\ell = k^{3/2}/\varepsilon$$

Constants that appear in the two turbulence equations are c_1, c_2, c_μ, σ_k, and σ_ε. Values used in the computer program together with their Fortran symbols are given in Table III.

TABLE II

VARIABLE FUNCTIONS (Table I of Ref. 15)

ϕ	a_ϕ	b_ϕ	c_ϕ	S_ϕ
ω/r	r^2	r^2	μ_{eff}	0
ψ	0	$1/\rho r^2$	1	$-\omega/r$
k	1	μ_{eff}/σ_k	1	$-(G-\rho\varepsilon)$
ε	1	$\mu_{eff}/\sigma_\varepsilon$	1	$-(c_1 G\varepsilon/k - c_2\rho\varepsilon^2/k)$
T	1	μ_{eff}/σ_h	1	0

G is a generation term:

$$G = \mu_{eff}\{2[(\frac{\partial V_z}{\partial z})^2 + (\frac{\partial V_r}{\partial r})^2 + (\frac{V_r}{r})^2] + [\frac{\partial V_z}{\partial r} + \frac{\partial V_r}{\partial z}]^2\}$$

TABLE III

TURBULENCE CONSTANTS (Table II of Ref. 15)

Constant	c_1	c_2	c_μ	σ_k	σ_ε
Fortran Symbol	C1	C2	CMU	PR(NK)	PR(NE)
Value	1.45	2.0	0.09	1.0	1.3

Boundary conditions are specified at every point on the boundary. Wall functions that are derived from Couette flow solutions are used in evaluating boundary values for ω/r, k, ε, and T. Other boundary conditions are given in Figure 9.

The computer program calculates heat and momentum transfer in steady two-dimensional axisymmetric recirculating flows. Five simultaneous coupled non-linear partial differential equations are solved. The finite difference equations are implicit equations that are coupled and non-linear. The Gauss-Seidel point iterative method is used to solve the finite difference equations. Provisions are made for both overrelaxation and underrelaxation of the variables.

References 14 and 15 contain a more complete discussion of the mathematical formulation of the problem, development of the finite difference equations, and solution algorithms. An excellent discussion of several turbulence models can be found in Reference 16.

The boundary conditions on the pipe wall can be changed so that the effect of mass addition through the wall for non-reacting flows can be investigated analytically. A constant radial velocity at the wall, which yields a linearly varying stream function along the wall, is used to simulate wall mass injection (See Figure 10). In this initial study, the main flow and the wall mass addition were identical in chemical composition and temperature.

In Pistep II, wall functions based on Couette flow are used to specify the boundary conditions on the pipe wall for all of the variables except stream function. For very low blowing rates, which are characteristic of solid fuel ramjets, Couette flow solutions may yield realistic results. However, for higher mass injection rates, Couette flow solutions may not adequately represent the boundary conditions.

The centimeter-gram-second system of units is used in the Pistep II computer program.

VI. RESULTS AND DISCUSSION

A. COLD FLOW EXPERIMENTS

A series of cold flow visualization tests were conducted to determine the reattachment point location for flow over a rearward facing step at the inlet of a cylindrical tube. Defining a step Reynolds number as:

$$Re_{step} = \frac{\rho V h}{\mu} \quad \text{where}$$

ρ... fluid density

V... average velocity in the port of the tube

h... step height

μ... fluid viscosity

it was found that the reattachment point location remained constant as the step Reynolds number was changed for a given step height. The reattachment point moved further downstream with increasing step height. The tube inside diameter was used to non-dimensionalize the reattachment point location from the face of the step. A linear least-square curve fit of 47 data points was used to obtain the following equation (See Figure 11).

$$\frac{x_r}{D} = 7.15\ (h/D) + 0.35$$

Figure 12 compares the data obtained in this investigation with the data of Abbott and Kline [Ref. 1] and Krall and

Sparrow [Ref. 2]. The unsymmetric reattachment points obtained by Abbott and Kline are shown. The flow reattached at different locations on either side of the two-dimensional channel. The location of the maximum heat transfer coefficient found by Krall and Sparrow for water flow through an orifice in a cylindrical tube was used to locate the reattachment point data shown in Figure 12.

The data from this study fell between that of Krall and Sparrow and the downstream reattachment point found by Abbott and Kline. Air was used in this study whereas water was used in the other studies; however, each study found that reattachment point location was not affected by changing Reynolds number for a constant step height. Krall and Sparrow also found that changing Prandtl number of the flow did not change the reattachment point location.

The spread in the cold flow data in Fig. 11 is probably due to larger relative errors in measurement closer to the step face and not due to Reynolds number effects.

At higher step Reynolds numbers small vortices were observed at the step face similar to the observations of Abbott and Kline for two-dimensional channel flow. The reattachment point was axially symmetric for most Reynolds number flows. However, at high Reynolds numbers the reattachment point varied around the circumference of the tube. Four distinct lobes could be seen when this occurred and may be associated with the small vortices at the step face. It

was also observed that the rotation and mixing of the flow in the recirculation zone became more intense as the height of the step increased.

B. PISTEP II RESULTS

The Pistep II computer program was run for four step configurations and five inlet velocities. Table IV summarizes the reattachment point results. A linear least-square curve fit is shown in Figure 11 and Figure 12 for comparison with the cold flow data and the data from other investigations. From these figures it is seen that Pistep II gives a dependence of X_r/D on h/D which is in general agreement with experimental results. With the current turbulence model and wall functions, the results agree closely with those of Krall and Sparrow and fall somewhat below the data obtained in this investigation.

A 21 x 21 grid was used for the h/D of .25 and a grid of 20 x 20 was used for the other values of h/D. The computing time required for each run was on the order of 20 to 30 minutes. Underrelaxation of the variables was required to ensure numerical stability. Even with underrelaxation, the case with h/D of 0.421 was numerically unstable for most of the inlet velocities tried. However, this case converged the fastest when numerically stable.

At each of the grid points, Pistep II calculated the distribution of the following parameters: vorticity, stream function, turbulent kinetic energy, turbulence dissipation

TABLE IV

RESULTS OF PISTEP II CALCULATIONS

h/D	X_r/D	Re_{step}*	Niter**	V_{in}(cm/sec)
.250	1.735	2446	900	1524
.250	1.696	12232	700	7620
.250	1.761	24465	900	15240
.250	1.702	36698	700	22860
.289	1.979	2009	800	1524
.289	2.008	20089	800	15240
.289	2.004	31033	800	22860
.342	2.152	1335	700	1524
.342	2.199	6677	800	7620
.342	2.161	13354	700	15240
.342	2.215	20032	800	22860
.421	2.705	4109	523	15240
.421	2.708	6163	521	22860

* Based upon a fixed laminar viscosity of 1.78×10^{-4} gm/cm.sec

** Niter is the number of iterations

rate, non-dimensional temperature, axial velocity, radial velocity, effective viscosity, density, and turbulence length scale. Variations of shear stress and heat transfer coefficient along the walls were also calculated. The location of the flow reattachment point was determined by solving for the point at which the wall shear stress was zero.

C. PISTEP II WITH WALL MASS ADDITION

The boundary conditions were altered along the "north" wall as shown in Figure 10. A linearly varying stream function (i.e., a constant radial velocity at the wall) was used to simulate injection of mass uniformly through the wall. For this initial study, the chemical composition of the mass injected through the wall was chosen to be identical to that of the main stream coming in the inlet. FAR is a term that is analogous to a fuel air ratio, and represents the fraction of the total incoming inlet stream that is injected through the wall. For example, FAR = 0 gives no wall mass injection. FAR = 0.5 gives an amount of wall mass injection equal to half of the inlet stream so that the amount leaving at the exit is 1.5 times the amount entering at the inlet.

FAR was varied in increments of 0.1 for the case in which inlet velocity was 500 ft/sec (VIN = 15240 cm/sec) for an h/D of 0.342. Stream function output was punched onto cards which were used as input for a separate program

which generated contours of streamlines using the Calcomp plotter (see Appendix A). Figures 13 through 21 show the streamline patterns obtained for various conditions. It should be noted that the streamline patterns are shown only for the upstream half of the ramjet and that the radial coordinate has been expanded more than the axial coordinate so that the figures are not to scale. This permits a better visual presentation of the streamlines in the recirculation zone. Note that with wall mass addition (Figures 14 through 18), a streamline that originates on the north wall in the recirculation region escapes from the recirculation zone and enters the main stream of flow. Figures 20, 13, and 19 show the effect of increasing step size (h/D) while maintaining inlet velocity constant (mass flow rate decreases). Comparison of Figures 20 and 21 shows the effect of decreasing inlet velocity (or inlet mass flow) with a fixed h/D and comparison of Figures 13 and 21 shows the effect of decreasing step size with a fixed inlet mass flow rate.

Table V summarizes the results for wall mass addition. The reattachment point location, based on the point where wall shear stress is zero, moves upstream slightly as wall blowing is increased. The "wall shear stress" is calculated from the stream function difference between the wall node and the first node out from the wall. In the tube between these two nodes the axial velocity is at least an order of magnitude greater than the radial velocity. This permitted the calculation of the "reattachment point" in the same

manner as for no blowing. Also, the magnitude of the radial velocity at the wall is quite small compared to the magnitude of the inlet velocity. It should be emphasized that these results were obtained using the same boundary conditions on ω/r, T, ε, and k as for no blowing. Further studies are required to determine whether or not this assumption is realistic.

TABLE V

PISTEP II WITH WALL MASS ADDITION (h/D = 0.342)

V_{in}(cm/sec)	FAR	x_r/D	V_{wall}(cm/sec)
15240	0.0	2.211	0.0
15240	0.1	2.191	4.7
15240	0.2	2.168	9.5
15240	0.3	2.145	14.2
15240	0.4	2.123	19.0
15240	0.5	2.101	23.7

Note: 900 iterations for each of the above runs

D. PMM/AIR RAMJET

Seventy-four hot firing tests were conducted. A Fortran language computer program was written to reduce the data. A computer listing together with the output is included in

Appendix B. The first three pages of the output tabulate the measured data for each test in which combustion was sustained. This is followed by the calculated results. This program was modified to reduce the data for the tests in which combustion was not sustained. A computer listing and output for the non-sustaining tests is included in Appendix C.

The expected uncertainties in the experimental results was calculated using the error analysis method of Kline and McClintock [Ref. 17]. Using the notation defined in the ramjet data reduction computer program, the uncertainties are given in Table VI.

The step inlet caused non-uniform regression of the fuel grains. There was less regression of the fuel at the head end in the recirculation region, and nearly uniform regression downstream of the reattachment point, where regression rate was observed to decrease slightly with increasing distance from the head end. The inlet effect was more pronounced for larger values of h/D. For the majority of the tests there was a significant amount of carbon deposited on the surface of the fuel at the head end. The reattachment point locations were measured to the edge of the carbon deposits or to the location of maximum regression. These two locations were nearly coincident in most cases. The regression patterns for three tests are shown in Figure 22.

Regression rates were calculated using two methods. Based upon the exit diamter, average regression rate can

TABLE VI

ERROR ANALYSIS

Symbol	% Error	Variable
WDOT	6.3	air weight flow rate
TC	13.8*	calculated chamber temperature
RDE	1.4	$\dot{r}$ based on exit diameter
RWT	1.1	$\dot{r}$ based on weight loss
WF	.6	fuel weight flow rate
FG	8.6*	gross thrust
FISP	8.6*	fuel specific impulse
RESTEP	5.8	step Reynolds number
GAIR	5.7	air flux rate
UPORT	15.0*	average port velocity
SFC	8.6*	specific fuel consumption
EQN	11.0	empirical $\dot{r}$ equation

* The uncertainty in the ratio of specific heats, γ, and the gas constant, R, were not included in this analysis. Complete expansion through an ideal nozzle was assumed in calculating FG, FISP, and SFC.

be defined by:

$$\dot{r} = \frac{d_f - d_i}{2\ \Delta t} \quad \text{(in/sec)}$$

where d_i and d_f are the initial and final exit diameters before and after firing, and Δt is the burn time. An average regression rate based on weight loss of the fuel can also be calculated:

$$\dot{r} = \frac{\sqrt{\frac{4\ (W_i - W_f)}{\pi\ \rho\ L} + d_i^{\,2}} - d_i}{2\ \Delta t} \quad \text{(in/sec)}$$

where W_i and W_f are the initial and final weights of the grain, ρ is the density of the fuel, and L is the grain length. This expression for the regression rate gives a better average value when there is non-uniform regression along the length of the grain, and was used throughout this investigation.

The dependence of the regression rate of the fuel on chamber pressure, P (psia), inlet air temperature, T (°R), and average mass flux of air, G ($lbm/in^2 sec$), was determined by holding two of these parameters at fixed values and varying the third for several tests. It was found that the regression rate varied as:

$$\dot{r} = C\ P^{0.51}\ T^{0.34}\ G^{0.41} \quad \text{(in/sec)}$$

where C is a proportionality constant. For a step h/D of 0.333, $C = 2.3 \times 10^{-4}$ and for a step h/D of 0.416, $C = 3.4 \times 10^{-4}$. A plot of the regression rate based on weight loss, $\dot{r}_{wt}$, versus this empirical regression rate equation is shown in Figure 23. On the sixth page of the ramjet data reduction computer program output in Appendix B, the numerical results are tabulated. The expected uncertainty in the empirical equation was calculated to be 11%.

Muzzy [Ref. 4] has shown that the regression rate equation for a hybrid rocket operating in the kinetically dominated region can be expressed as:

$$\dot{r} = C\, P^{0.5}\, G^{a}\, X^{b}$$

where a varies from 0.3 to 0.4 and b varies from -0.1 to -0.2, and X is the longitudinal coordinate.

Thus, the average regression rate of the fuel in a solid fuel ramjet is very similar to that for pressure sensitive hybrid rocket combustion. This is not surprising since the reattachment point normally occurred at less than one-fourth

of the grain length. Aft of the reattachment point combustion should approach that of a kinetically controlled hybrid combustor.

The maximum regression rate of the fuel occurred near the location of the flow reattachment point. This is due to several factors. More oxidizer reaches the wall from the impingement of the main oxidizer stream at the reattachment point. In addition, the maximum Nusselt number occurs near the reattachment point location.

Data from 36 of the tests in which combustion was not sustained are tabulated with the computer program in Appendix C. For the smallest step h/D used (0.25), combustion was sustained only while the ignition system was operating. As soon as ignition was terminated, the flame blew off. For the middle step (h/D = 0.333) the flame blew off as soon as the air flow was activated for many of the tests at higher flow rates. Some of the tests in which combustion was not sustained may have been due to insufficient ignition prior to activating the air flow.

Tests performed at the United Technology Center [Ref. 8] have indicated that inlet configuration is more important in determining when combustion will be sustained. A critical step h/D ratio was found to be the best criterion. For values of h/D less than the critical value, combustion could not be sustained. It was reported that for one particular all-hydrocarbon fuel the critical h/D was 0.14. For polymethylmethacrylate they found that the critical h/D

was 0.31. This criterion did not vary with step Reynolds number.

The data from this investigation indicated that for high inlet velocities with h/D greater than the critical value determined by UTC, combustion may not be sustained. It appears that not only is h/D important, but inlet velocity, ignition time, and inlet temperature may also be important. At identical air mass flow rates, some of the tests at higher inlet temperatures failed to sustain combustion. This is probably a velocity effect since at constant mass flow rates, increasing temperature increases the velocity.

The Pistep II results, although for non-burning cases, should indicate trends to be expected in the burning tests. The data indicate that the magnitude of the velocity at a point in the recirculation zone is directly proportional to the inlet velocity. Also the velocity in the recirculation zone V, was found to be inversely proportional to h/D. Thus $V \propto VIN$ and $V \propto 1/(h/D)$. It was also found that $\frac{X_r}{D} \propto \frac{h}{D}$ but did not vary with inlet velocity.

A simplified model of the flame stabilization region is one in which the recirculation zone is considered as an ignition zone whose length, L, corresponds to the reattachment point location. At the flame blowoff condition, the gases traveling through the recirculation zone have an average contact time equivalent to the ignition time of the gases: $t_c = t_i$. If V is a characteristic velocity

in the recirculation zone, then $t_c \propto L/V$. Since

$$V \propto \frac{VIN}{h/D}$$

and

$$L \propto X_r/D \propto h/D$$

then one possible expression for contact time is

$$t_c \propto \frac{(\frac{h}{D})^2}{VIN}$$

The step h/D has a more dominant effect in determining flammability limits, however inlet velocity is also important. This treatment is oversimplified and was discussed only to indicate that the inlet velocity may be of significance in determining blowoff limits. In actuality, ignition time is a function of the fuel-air ratio in the recirculation zone and this is in turn a function of h/D. Thus, the functional form becomes more complex as one considers the details of the recirculation region.

It should also be noted that the simplified model described above neglects the effects of turbulence intensity on flame stabilization. Examination of Pistep II output indicates that for a constant inlet mass flow rate, increasing step height increases both the turbulent kinetic energy and

the turbulence dissipation rate. Also for a fixed inlet velocity, increasing step height decreases the recirculation zone velocity, the turbulent kinetic energy and the turbulence dissipation rate.

There are three blow-off situations to be considered. The first one is a steady-state blowoff limit that occurs when the mass flow rate in the recirculation zone is greater than the mass consumption rate by chemical reaction. The mass flow rate through the zone will depend upon the size of the zone and the velocity through the zone. This may be important in throttling applications during normal combustion. The second situation is one in which there are ignition transient blowoff limits during starting. Low chamber pressure during ignition gives higher inlet velocities which may cause the flame to blowoff even though combustion would sustain if ignition occurred at the expected operating pressure. Thirdly, it is possible that the flow at the step inlet may become choked at high mass flow rates when the chamber pressure is low during ignition. Subsequent expansion could modify the size and flow characteristics of the recirculation zone and cause the flame to blowoff. This indicates that if a ramjet operating with high flow rates could be started at a higher chamber pressure, combustion may be sustained.

The Pistep II computer program should prove to be advantageous in studying blowoff limits. When chemical reaction and wall mass injection are included in the

program, blowoff velocities in the recirculation zone could be realistically studied. The effect of h/D, inlet velocity (or mass flow rate), and chemical reaction rate could be considered. Blowoff limits have been calculated in this manner for premixed gases in a dump combustor [Ref. 15].

If the results of Abbott and Kline [Ref. 1] are similar to what may be expected in an axisymmetric situation with combustion, inlet turbulence would not be expected to affect the recirculation zone. However, inlet turbulence may affect the regression rate of the fuel downstream of the reattachment point. Further tests are needed to clarify the affects of inlet turbulence and distortion on solid fuel ramjet combustion.

VII. CONCLUSIONS

The cold flow visualization data were in general agreement with previous studies. Reynolds number had no measurable effect on the size of the recirculation zone and the reattachment point location. The reattachment point moved further downstream from the face of the step as step height increased.

The Pistep II computer program appears to predict with acceptable accuracy the reattachment point locations for non-reacting flows with no wall mass addition. Pistep II, modified for wall mass addition, indicated that the size of the recirculation zone and the reattachment point location are not greatly affected by wall mass addition. The location of the reattachment point moved slightly closer to the step face as wall blowing was increased. Experiments are required to verify this result, and the assumptions concerned with the boundary conditions used in the computer program require further investigation. The Pistep II computer program has proven to be accurate enough to warrant further development as a ballistics program for the recirculation region.

Solid fuel ramjets which use PMM as the fuel have an average regression rate that follows the expression: $\dot{r} = C\ P^{0.51}\ T^{0.34}\ G^{0.41}$. In addition, the maximum regression occurred near the reattachment point location. Downstream of the reattachment point the regression rate

decreased slightly with increasing distance from the head end. Thus, solid fuel ramjets have an average regression rate that closely follows the theoretical expression derived for kinetically controlled hybrid rocket combustion.

The step h/D is the dominant parameter in determining flame stability limits; however, inlet velocity is also an important parameter.

The results of this investigation indicate that a reasonable internal ballistics model for solid fuel ramjets may be obtained by using the Pistep II computer program (modified for chemical reactions and wall mass addition) together with the regression rate equation for kinetically controlled hybrid rocket combustion. The modified Pistep II program should be used to analyze the recirculation region (blowoff limits, etc.) and to provide the input data (chemical composition, etc.) to the regression rate equation for kinetically controlled hybrid rocket combustion. The latter should be employed downstream of the reattachment point.

VIII. SUGGESTIONS FOR FUTURE WORK

This work was an initial study of the internal ballistics of solid fuel ramjets. Additional experimental and analytical studies are required in order to a) obtain increased combustion efficiency, b) refine the internal ballistics model and c) study the effect of other inlet geometries and flow conditions on the regression rate of the fuel. Specific experimental studies needed include determination of a) the effect of wall mass addition on the recirculation zone for a step inlet using inert flows (to compare with the theoretical predictions using Pistep II), b) the effect of different inlet configurations such as swirl vanes and plug inlets on fuel regression rate and flame stability limits, and c) the effect of different mixing techniques on combustion efficiency. Analytical studies required are a) modifications to the Pistep II computer program to include chemical reaction with heat and mass transfer at the wall and b) combination of the recirculation zone model (as input) with the kinetically controlled hybrid combustion model to effect a usable internal ballistics model for solid fuel ramjets.

HIGHLY TURBULENT RECIRCULATION ZONE (MAY APPROACH A WELL-STIRRED REACTOR)

DIFFUSION FLAME LOCATED IN TURBULENT BOUNDARY LAYER WITH HIGH DEGREE OF OXIDIZER DILUTION

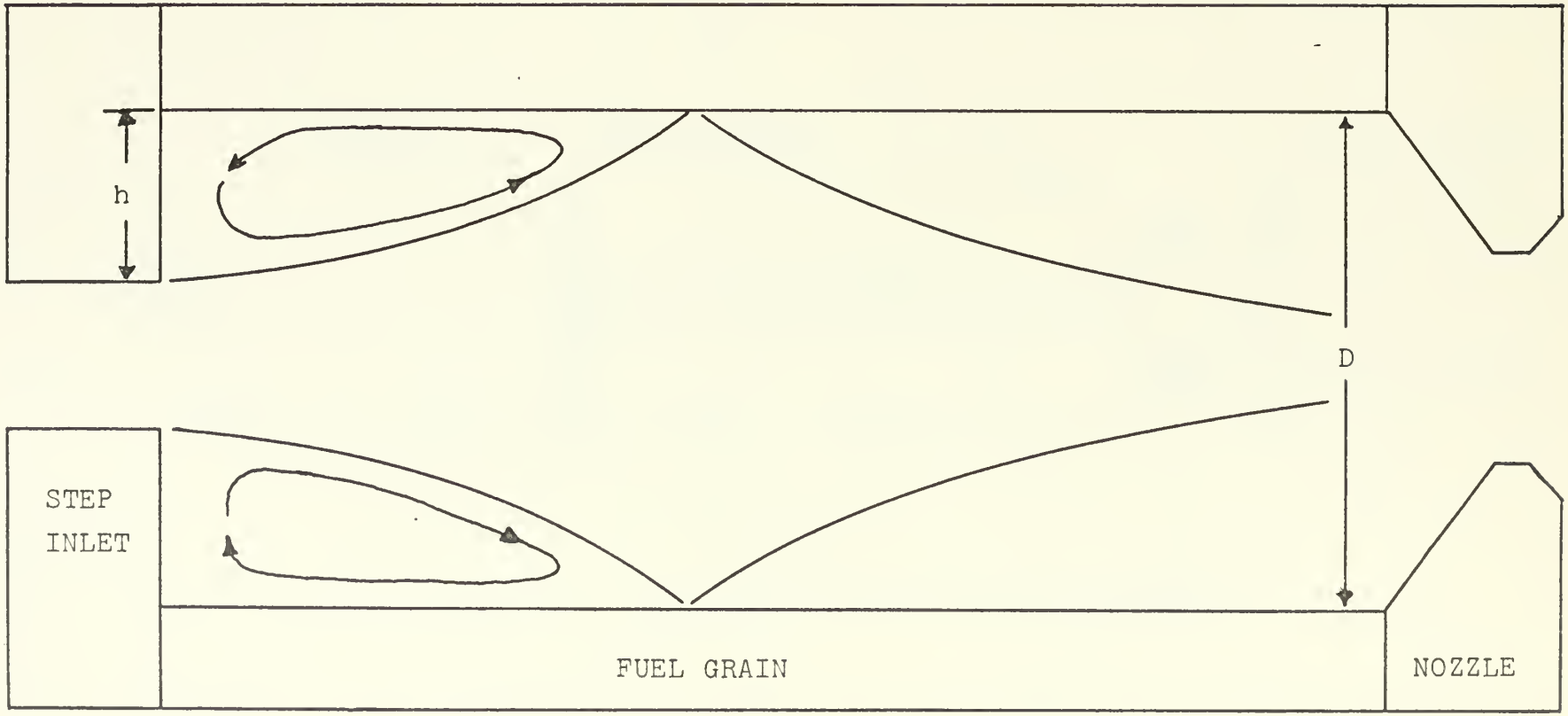

FIGURE 1. COMBUSTION MECHANISMS

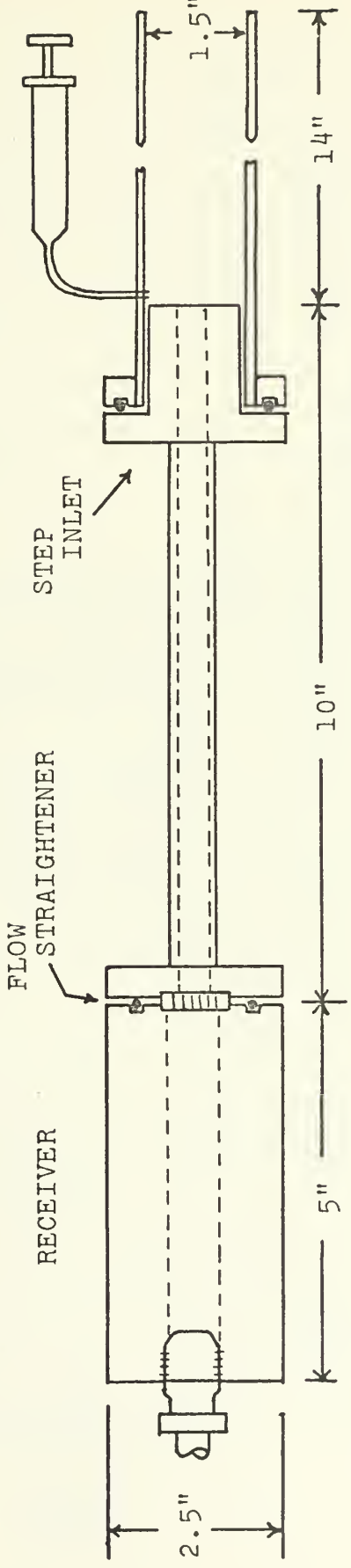

FIGURE 2. COLD FLOW VISUALIZATION APPARATUS

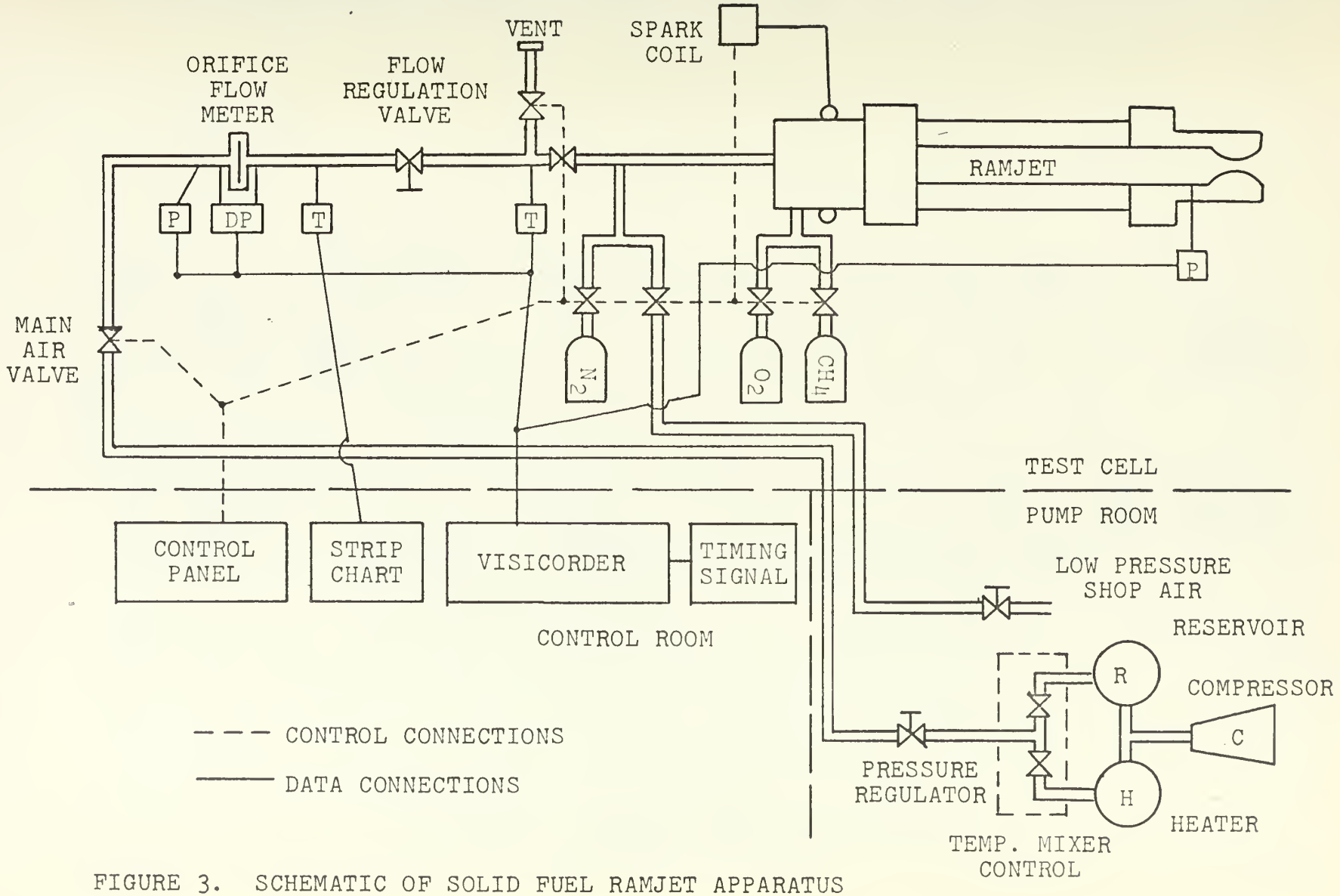

FIGURE 3. SCHEMATIC OF SOLID FUEL RAMJET APPARATUS

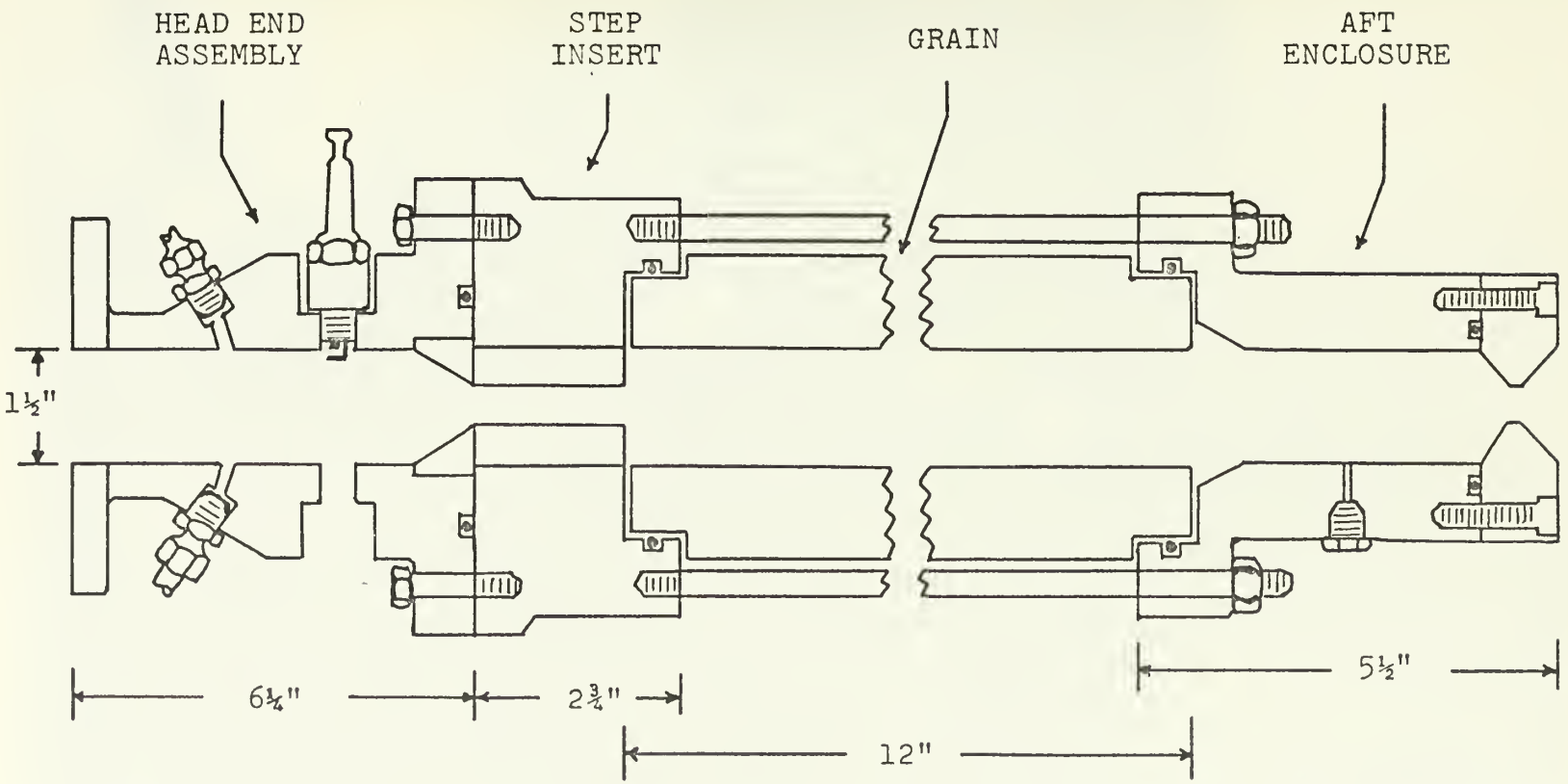

FIGURE 4. SOLID FUEL RAMJET MOTOR

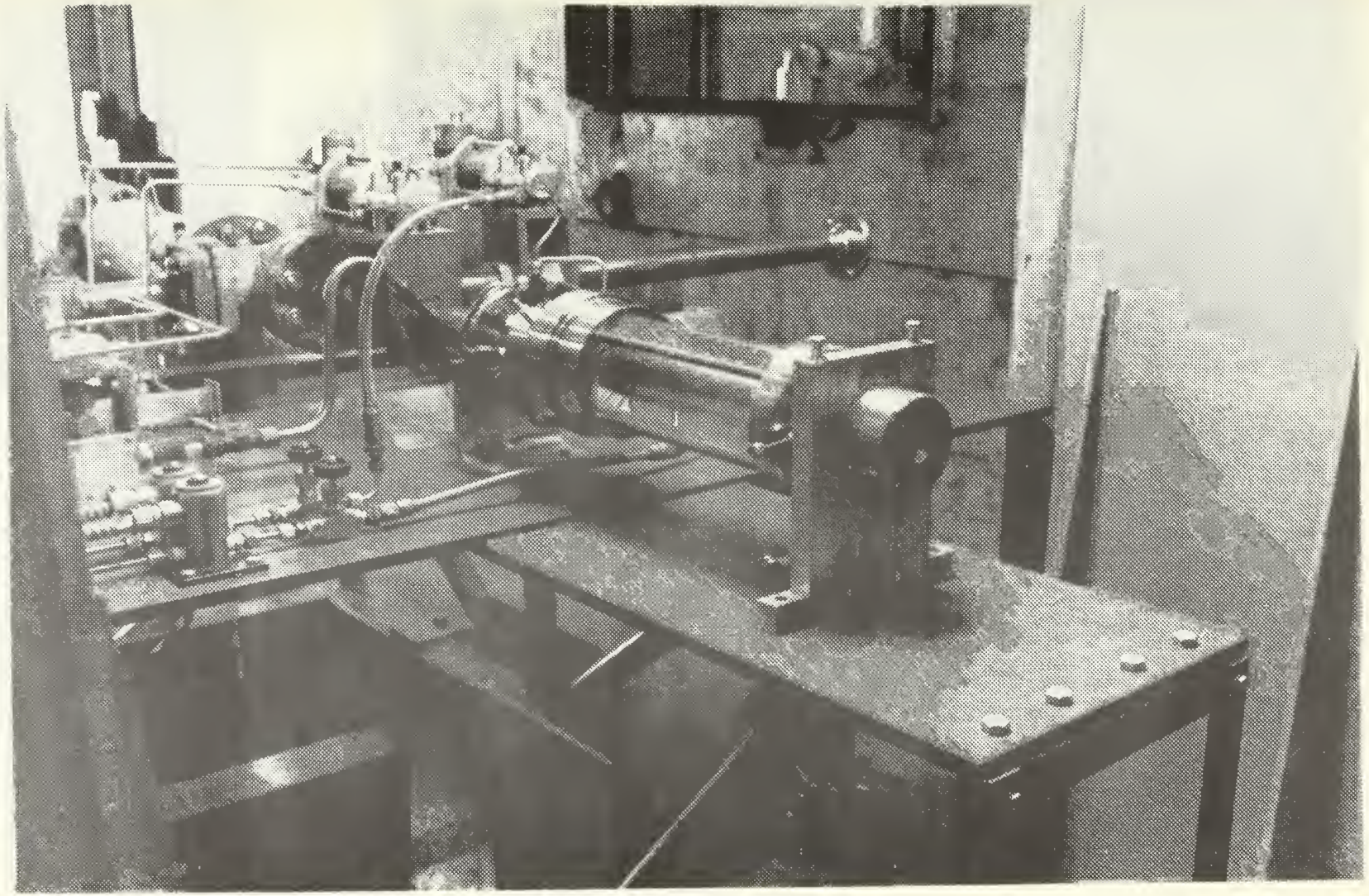

FIGURE 5. RAMJET MOTOR ON TEST STAND

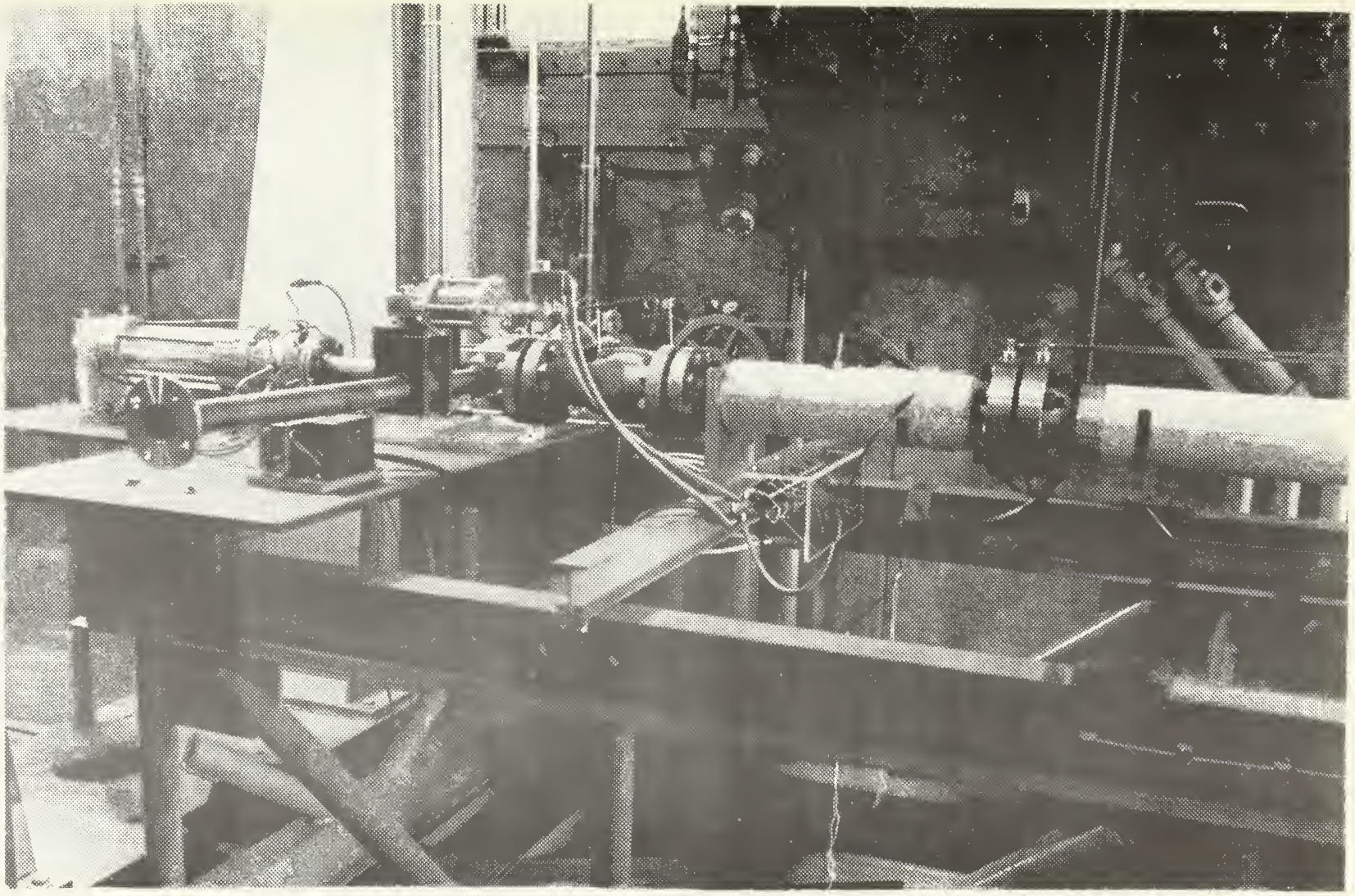

FIGURE 6. TEST STAND

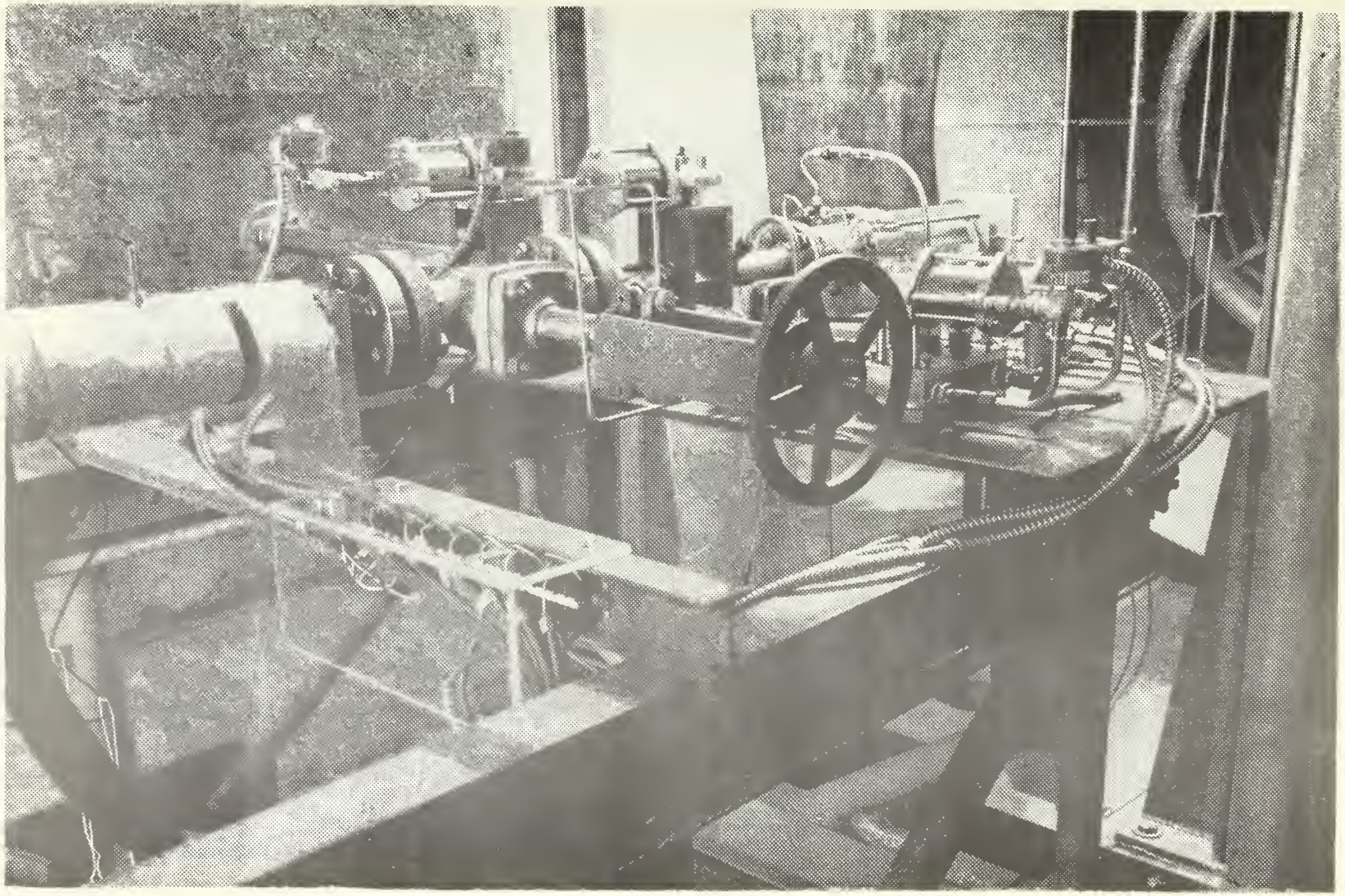

FIGURE 7. TEST STAND

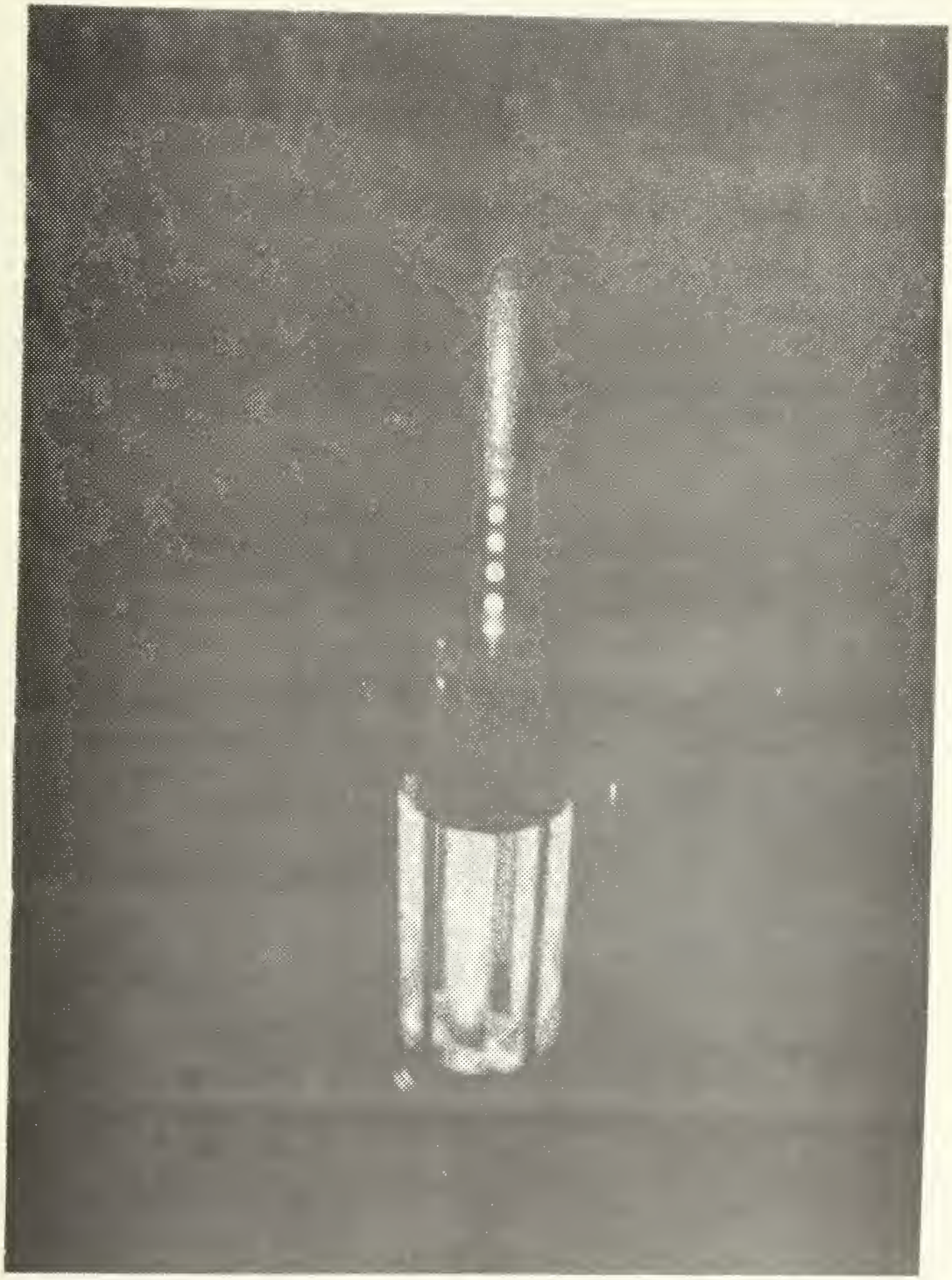

FIGURE 8. RAMJET MOTOR FIRING

NORTH WALL

$\psi = \psi_{wall}$ = constant

$T = 1$

$V_r = V_z = 0$

ω/r, k, ε calculated from wall functions

STEP WALL

$\psi = \psi_{wall}$ = constant

$\frac{\partial T}{\partial z} = 0$

ω/r, k, ε calculated from wall functions

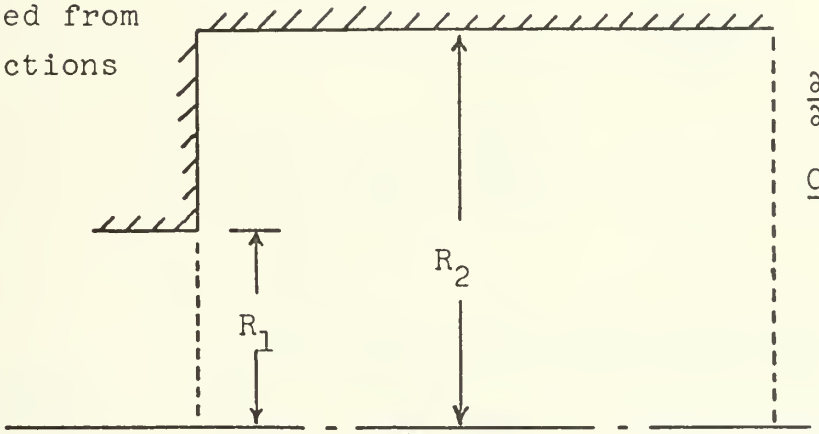

$\psi = \frac{\partial T}{\partial r} = \frac{\partial (\omega/r)}{\partial r} = 0$

INLET

$V_z = V_{in}$ = constant

ψ from $\frac{\partial \psi}{\partial r} = \rho r V$

$\omega/r = 0$

$k = 0.004\ V_{in}^2$

$\varepsilon = k_{in}^{3/2}/\ell$

$\ell = 0.05\ R_2(0.22)$

$T = 0$

$$T = \frac{t - t_{inlet}}{t_{wall} - t_{inlet}}$$

FIGURE 9. BOUNDARY CONDITIONS FOR PISTEP II (Figure 2 from Ref. 15)

NORTH WALL

$$FAR = \frac{\dot{M}_{wall}}{\dot{M}_{in}}$$

$$\dot{M}_{wall} = 2\pi R_2 L \rho V_r$$

$$V_r = \frac{FAR\ R_1^{\,2}\ V_{in}}{2\ R_2\ L}$$

$$\psi = \psi_{wall} + \frac{\dot{M}_{wall}\ z}{2\pi L}$$

$$\frac{\partial \psi}{\partial z} = \frac{\dot{M}_{wall}}{2\pi L} = \rho R_2 V_r = \text{constant}$$

$$T = 1$$

ω/r, k, ε — wall functions

STEP WALL

Same as Fig. 9

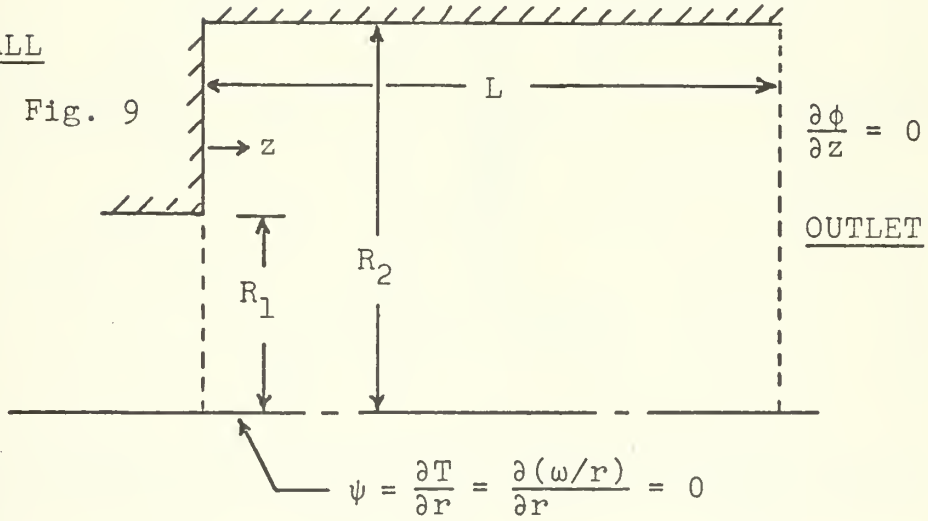

INLET

Same as Fig. 9

$$T = \frac{t - t_{inlet}}{t_{wall} - t_{inlet}}$$

FIGURE 10. BOUNDARY CONDITIONS WITH WALL MASS INJECTION

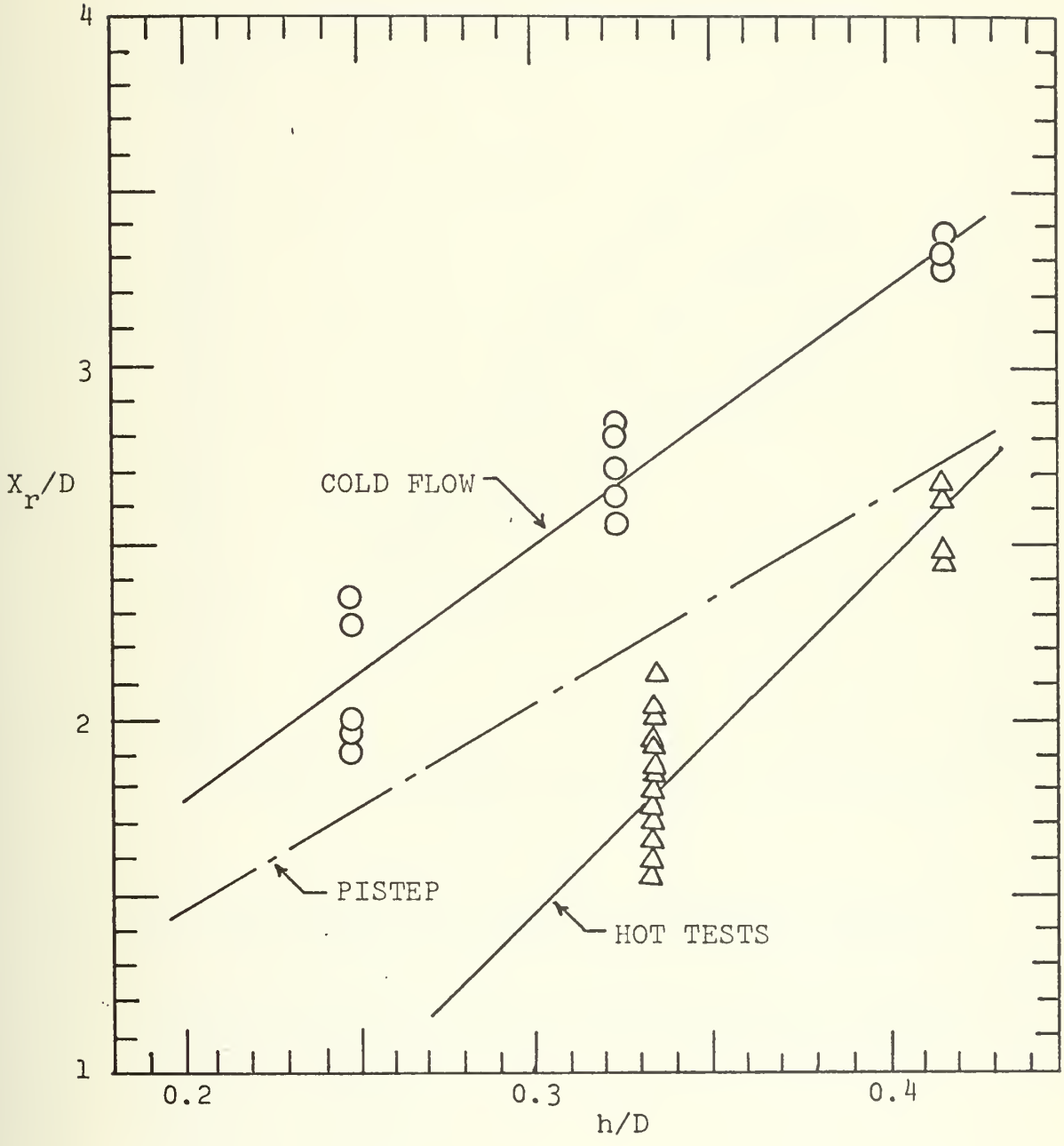

COLD FLOW: $X_r/d = 7.15(h/D) + 0.35$

PISTEP: $X_r/d = 5.54(h/D) + 0.36$

FIGURE 11. REATTACHMENT POINT VS. STEP HEIGHT

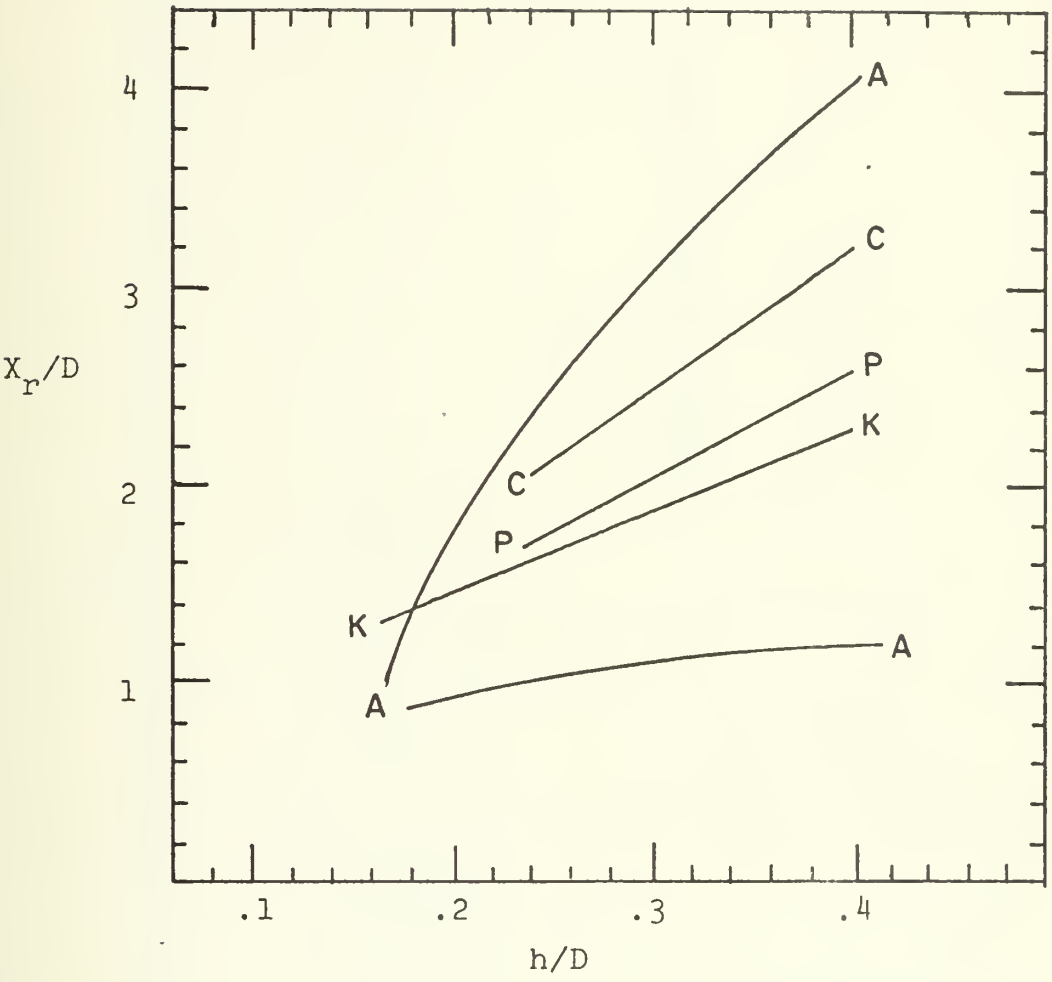

K—K Krall and Sparrow - based on location of maximum heat transfer coefficient (axisymmetric flow)

A—A Abbott and Kline - note different reattachment point locations for each side of two-dimensional channel

C—C COLD FLOW RESULTS

P—P PISTEP II RESULTS

FIGURE 12. REATTACHMENT POINT DATA COMPARISON

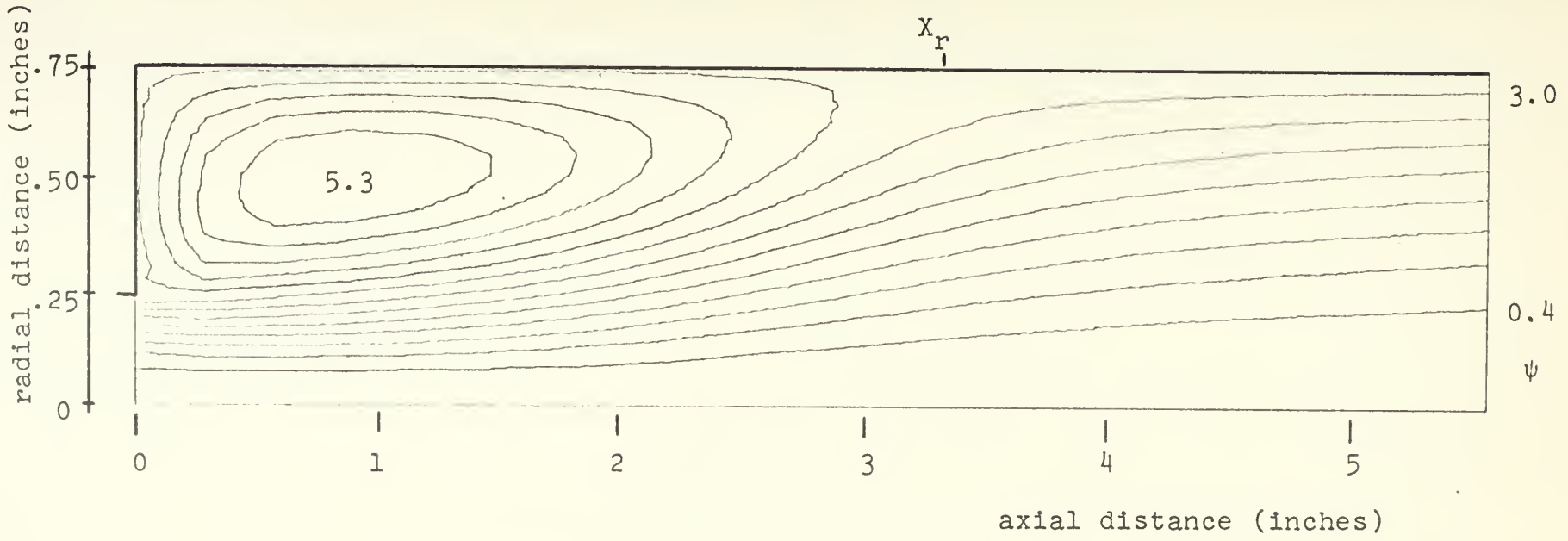

VIN = 15240

h/D = 0.342

X_r/D = 2.211

FAR = 0.0

FIGURE 13. STREAMLINES FOR NON-REACTING FLOW

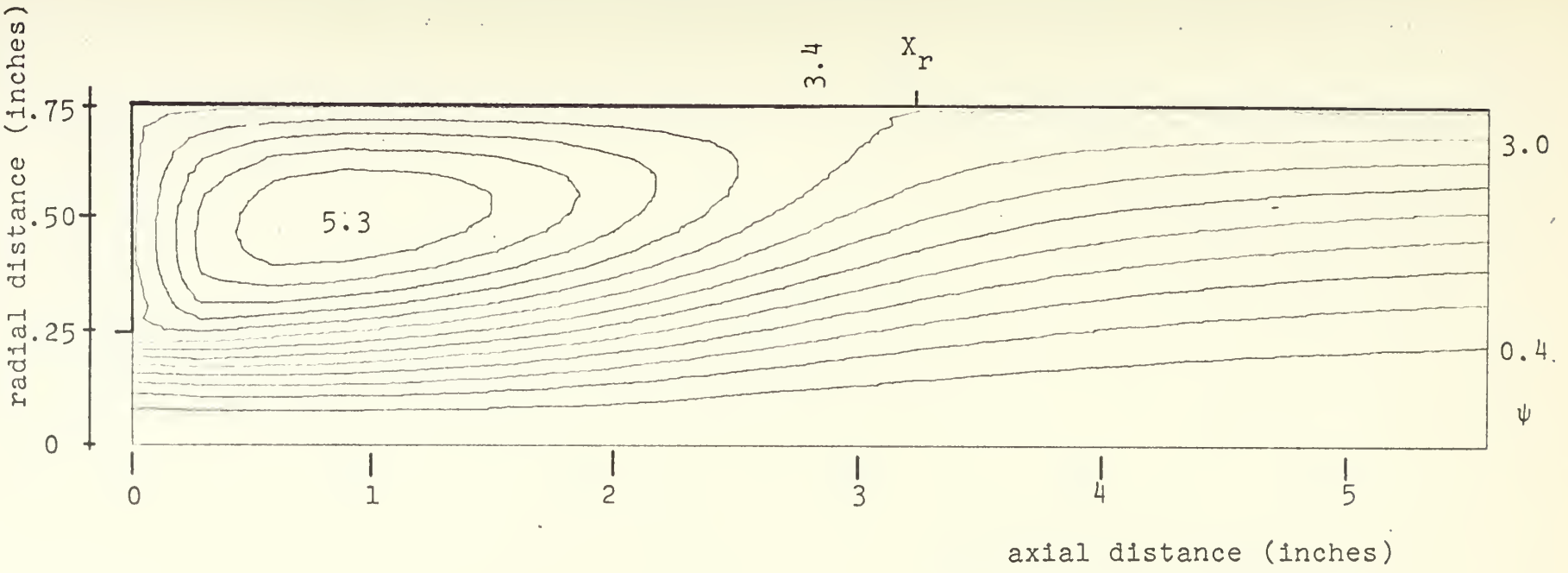

VIN = 15240

h/D = 0.342

X_r/D = 2.191

FAR = 0.1

FIGURE 14. STREAMLINES FOR NON-REACTING FLOW

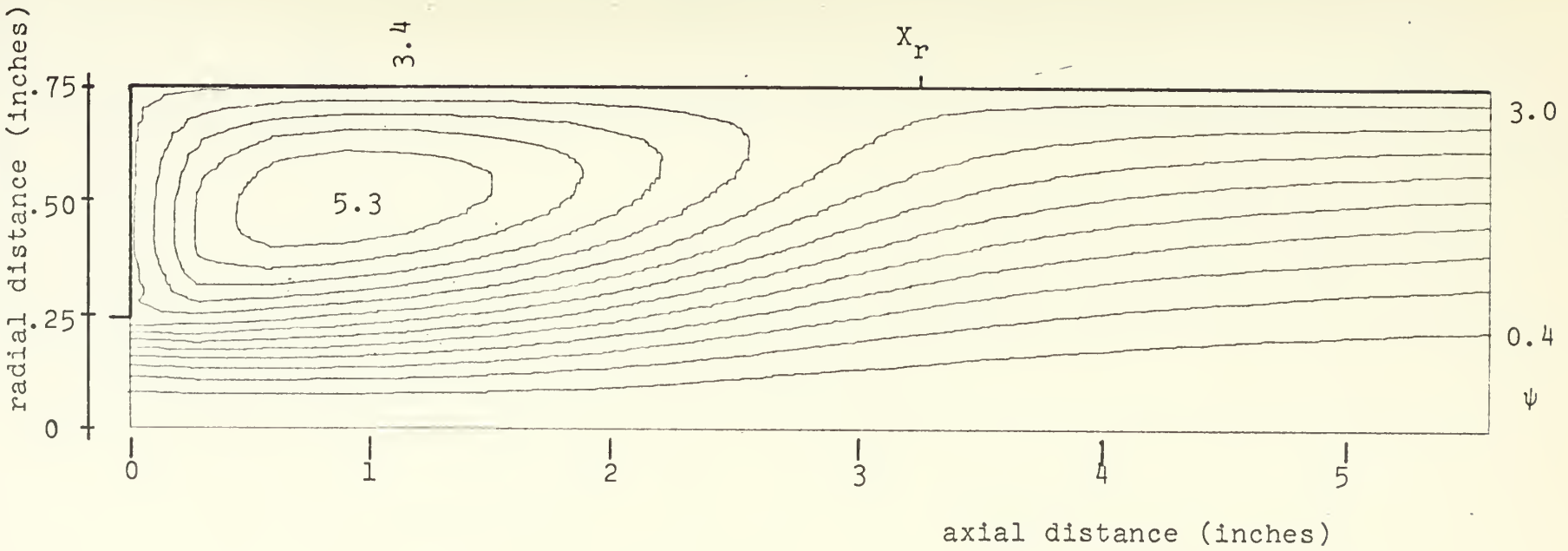

VIN = 15240

h/D = 0.342

X_r/D = 2.168

FAR = 0.2

FIGURE 15. STREAMLINES FOR NON-REACTING FLOW

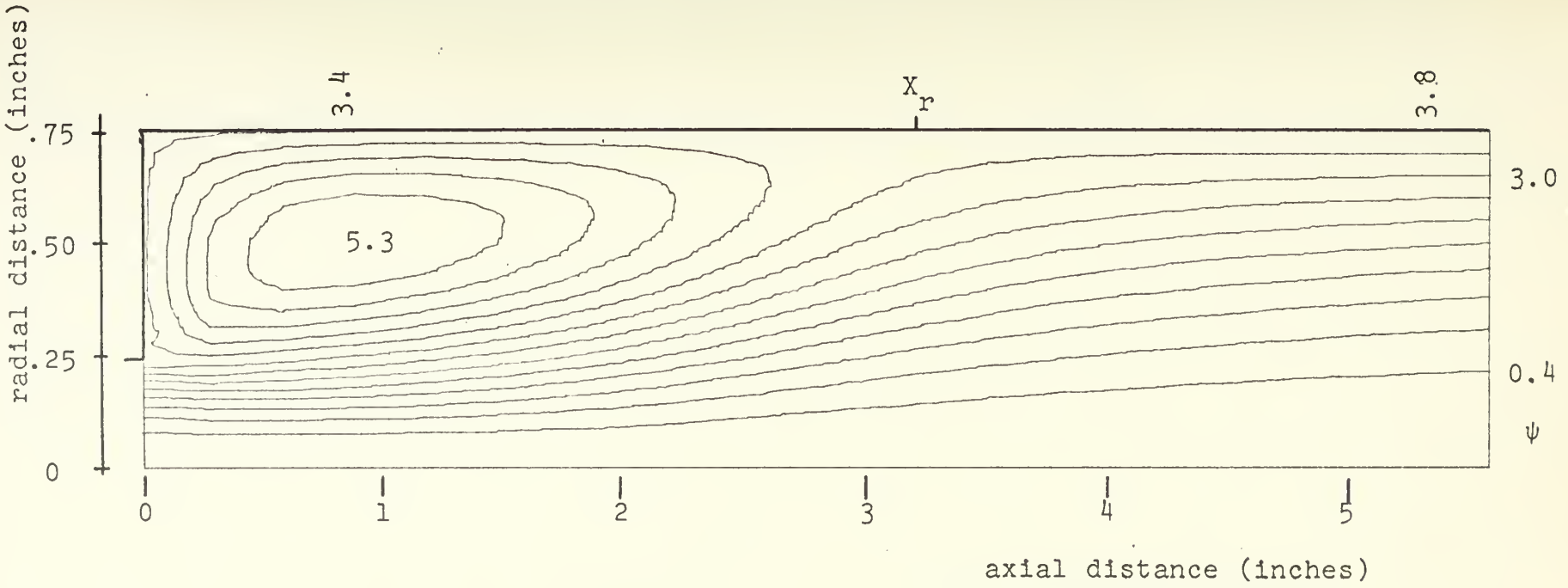

VIN = 15240

h/D = 0.342

X_r/D = 2.145

FAR = 0.3

FIGURE 16. STREAMLINES FOR NON-REACTING FLOW

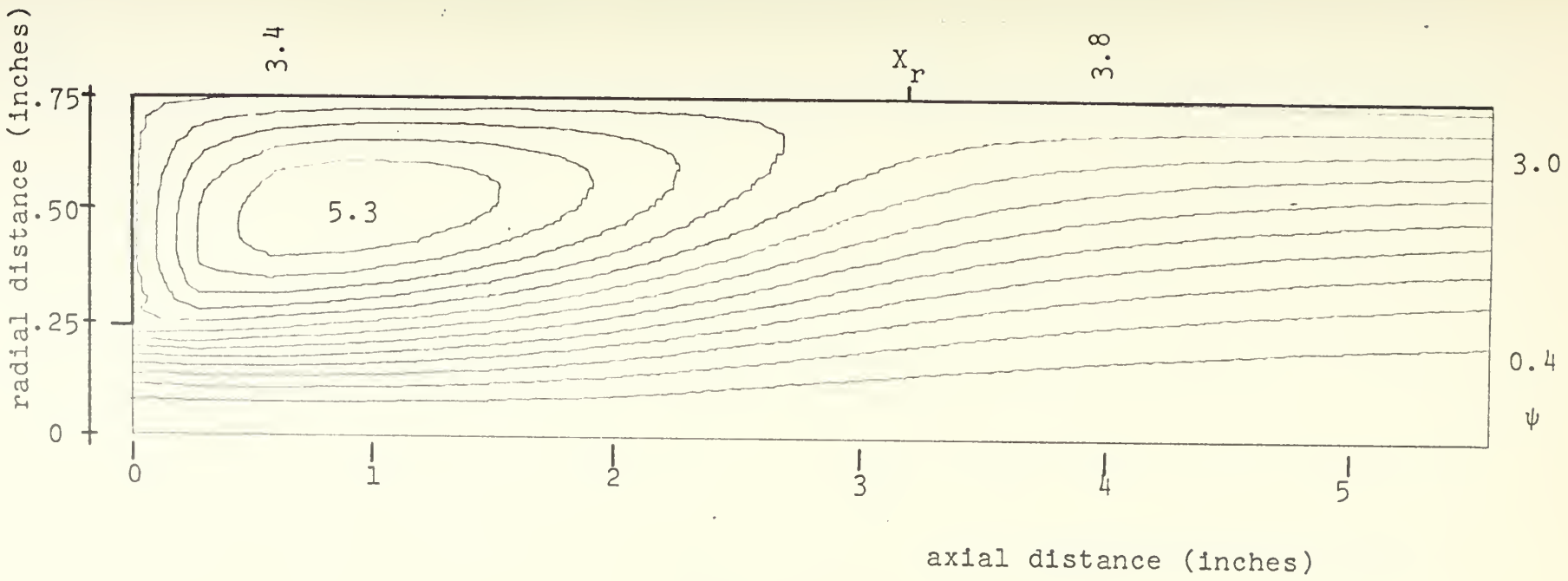

VIN = 15240

h/D = 0.342

X_r/D = 2.123

FAR = 0.4

FIGURE 17. STREAMLINES FOR NON-REACTING FLOW

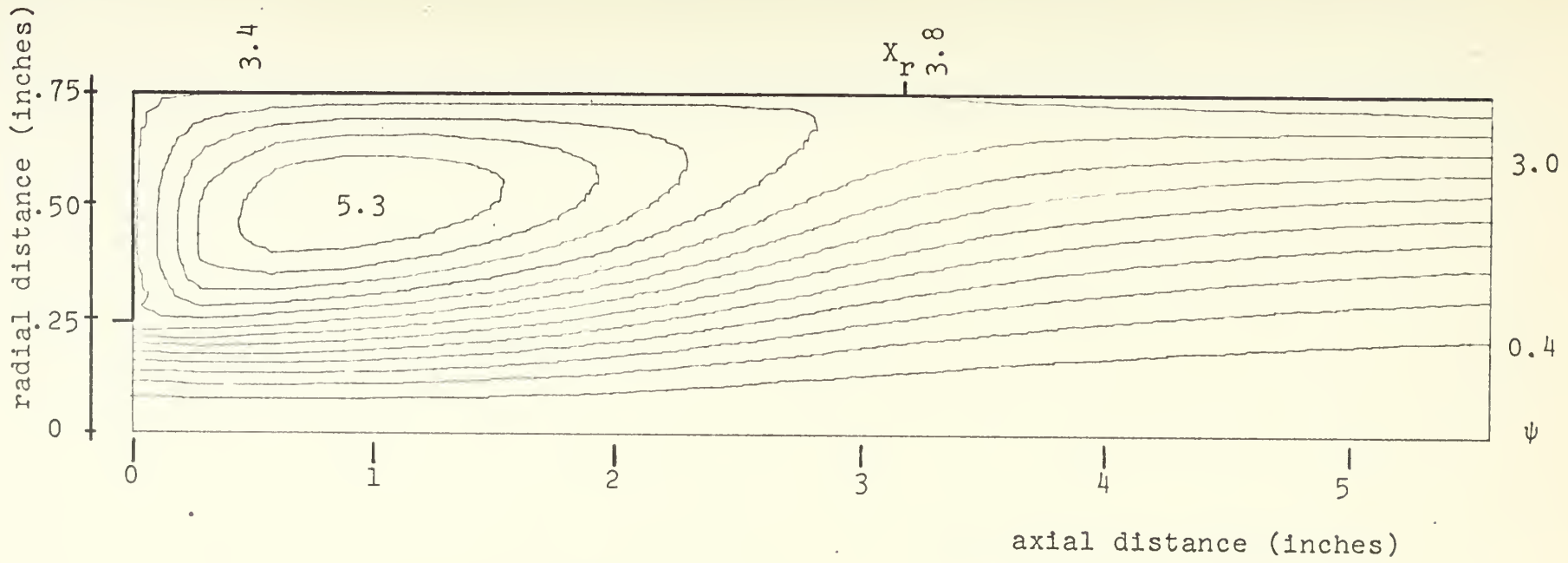

VIN = 15240

h/D = 0.342

X_r/D = 2.101

FAR = 0.5

FIGURE 18. STREAMLINES FOR NON-REACTING FLOW

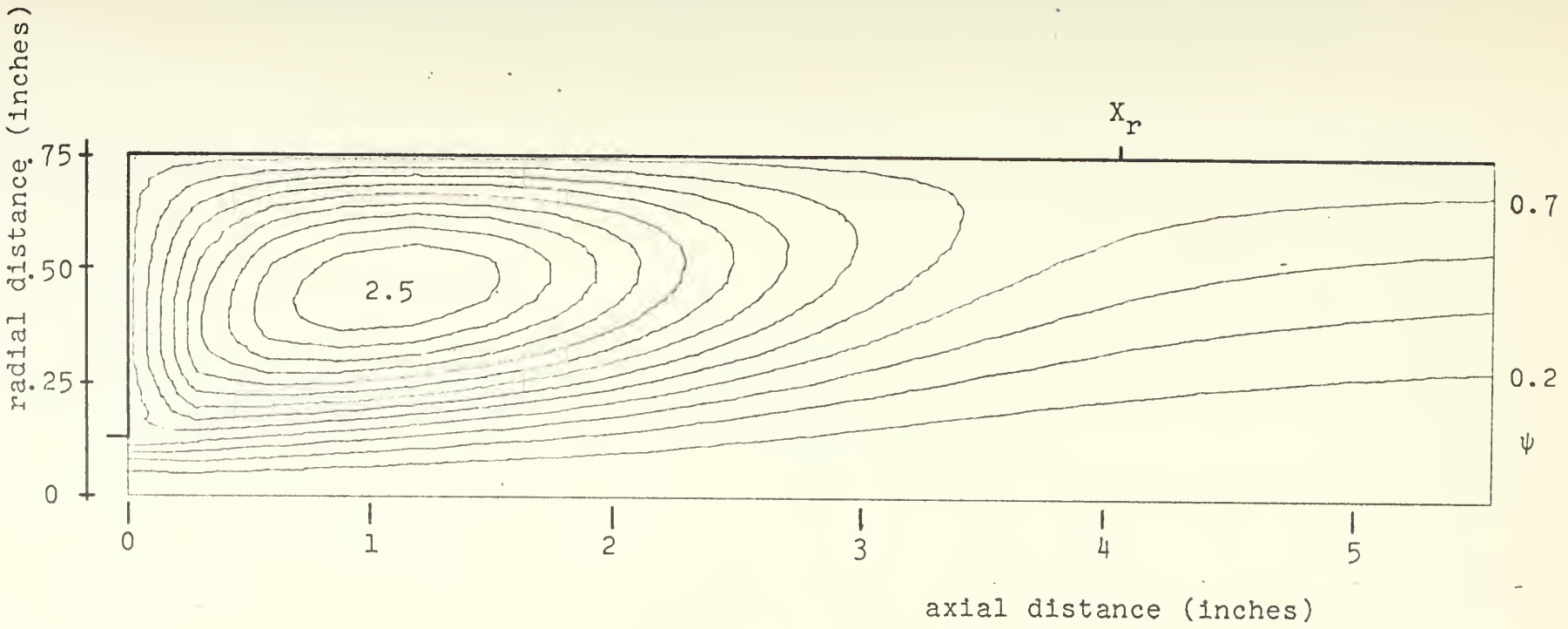

VIN = 15240

h/D = 0.421

X_r/D = 2.705

FAR = 0.0

FIGURE 19. STREAMLINES FOR NON-REACTING FLOW

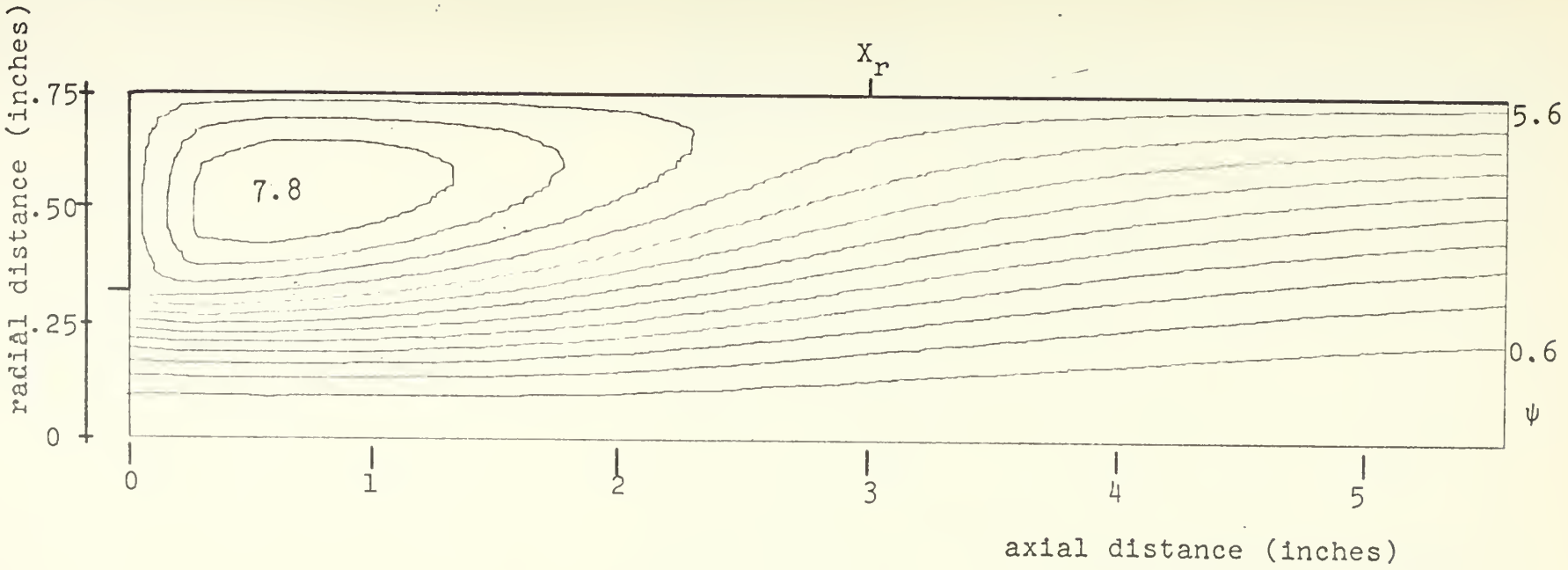

VIN = 15240

h/D = 0.289

X_r/D = 2.002

FAR = 0.0

FIGURE 20. STREAMLINES FOR NON-REACTING FLOW

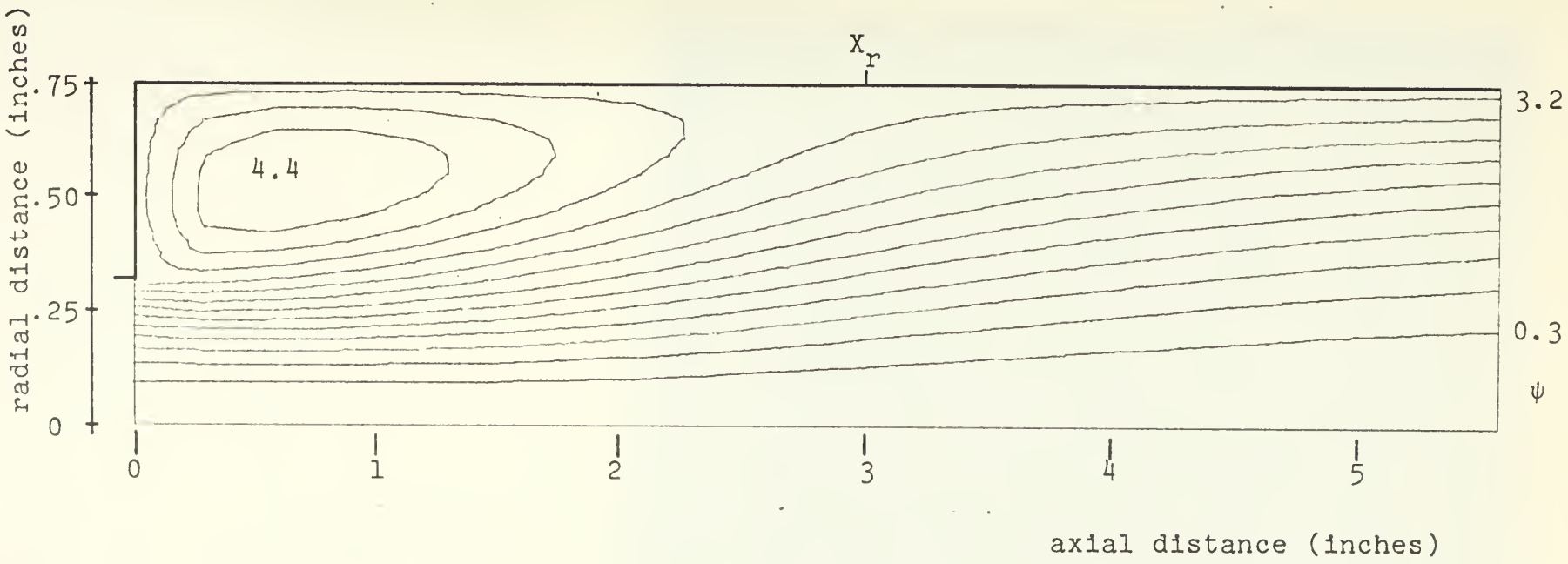

VIN = 8573

h/D = 0.289

X_r/D = 1.999

FAR = 0.0

FIGURE 21. STREAMLINES FOR NON-REACTING FLOW

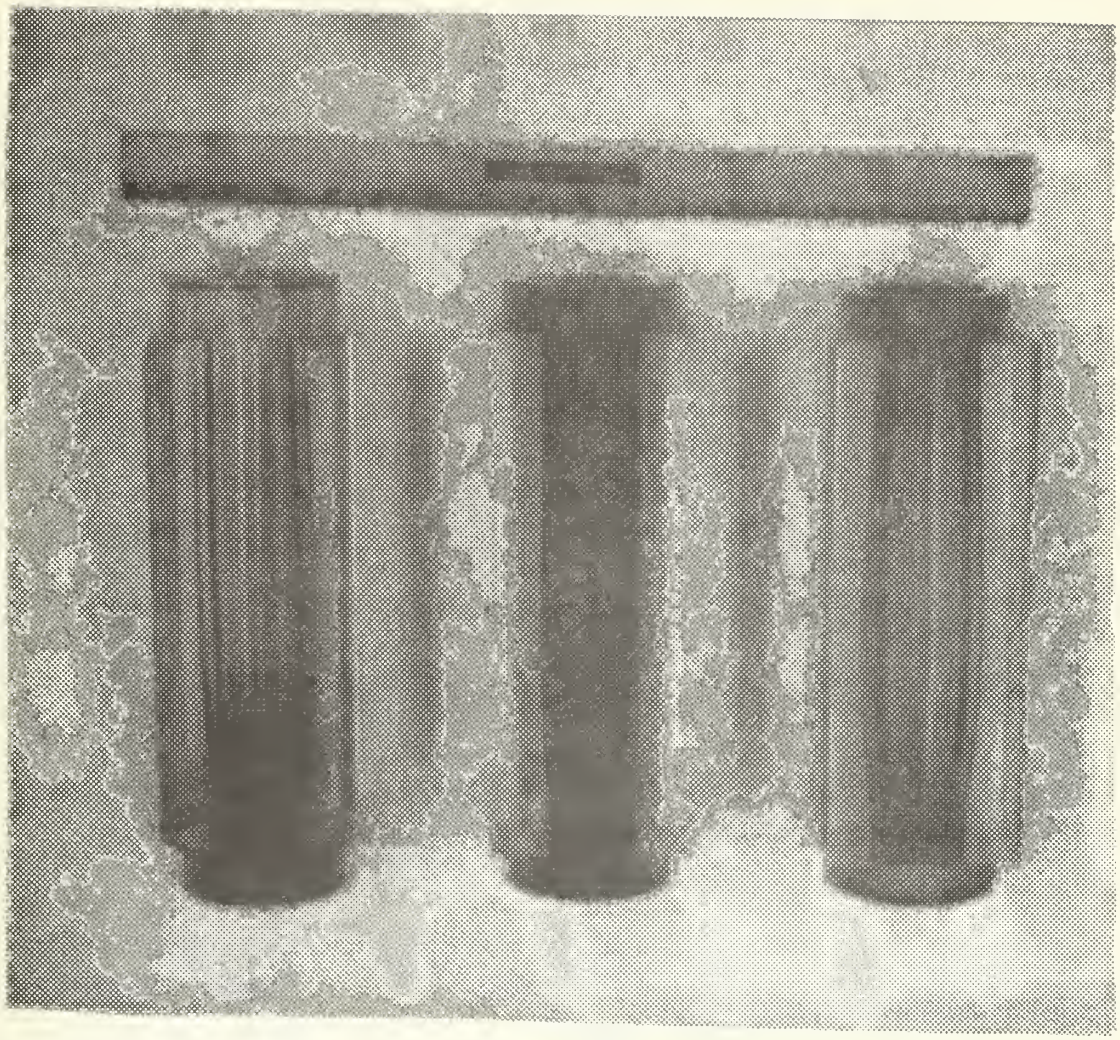

TEST	15	74	60
h/D	.33	.33	.41
P_c	62	55	71
T_{in}	66	320	203
G_{air}	.244	.074	.068
W_{air}	.43	.13	.12

FIGURE 22. REGRESSION PATTERNS

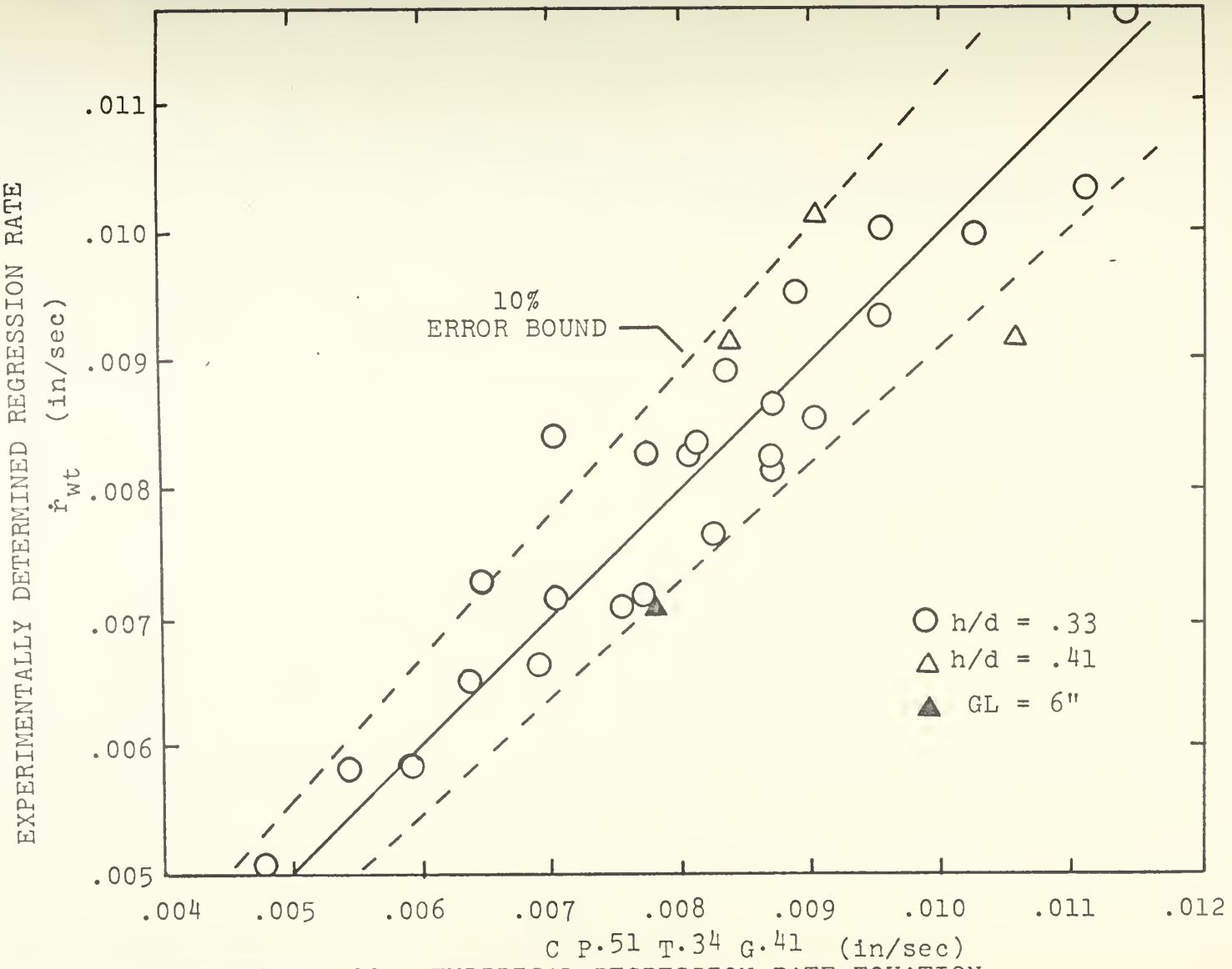

FIGURE 23. EMPIRICAL REGRESSION RATE EQUATION

APPENDIX A: PROGRAM TO CONTOUR STREAMLINES

```
C      COMPUTER PROGRAM TO TRANSFORM AND CONTOUR THE STREAM
C      FUNCTION OUTPUT FROM PISTEP II FOR VARIOUS WALL
C      BLOWING RATES.....BY L. D. BOAZ.
       DIMENSION AM(20,20),CL(15),AC(20,20)
       DIMENSION A(20,20),X1(20),X2(20),X1U(20),X2U(20)
       REAL*8 AA(20,20),U(20),V(20),YY(20),YI(20),X,Y,FXY
       REAL*8 PTITLE(12)/' STREAML','INES FOR',' COLD FL','OW IN SO','LID
      1 FUEL',' RAMJET ','L.D. BOA','Z   REAT','TACHMENT',' X/D=1.99','
      2      ','FAR=.0   '/
       LOGICAL*1 LTG(3)/.FALSE.,.FALSE.,.FALSE./
       DO 501 I=1,20
  501  READ(5,500)(A(I,J),J=1,10)
       DO 502 I=1,20
  502  READ(5,500)(A(I,J),J=11,20)
       READ(5,500)(X1(I),I=1,10)
       READ(5,500)(X1(I),I=11,20)
       READ(5,500)(X2(J),J=1,10)
       READ(5,500)(X2(J),J=11,20)
  500  FORMAT(10F8.4)
       READ(5,510) XRD,FAR
  510  FORMAT(2F8.4)
       DO 10 I=1,20
       U(I)=DBLE(X1(I))
       V(I)=DBLE(X2(I))
       DO 10 J=1,20
   10  AA(I,J)=DBLE(A(I,J))
C ****TRANSFORMING TO A UNIFORM GRID*****
       X1U(1)=0.
       DX1=X1(16)/19.
       DO 20 I=2,20
   20  X1U(I)=X1U(I-1)+DX1
       X2U(1)=0.
       DX2=X2(20)/19.
       DO 21 J=2,20
   21  X2U(J)=X2U(J-1)+DX2
       DO 30 I=1,20
       DO 30 J=1,20
       X=DBLE(X1U(I))
       Y=DBLE(X2U(J))
       N=20
       M=20
       DO 40 NR=1,N
       DO 41 NC=1,M
   41  YY(NC)=AA(NR,NC)
   40  CALL SPLIN1(V,YY,M,Y,YI(NR))
```

```
      CALL SPLIN1(U,YI,N,X,FXY)
      AC(I,J)=SNGL(FXY)
   30 CONTINUE
      IN=20
      JN=20
      WRITE(6,101)(X1(I),I=1,IN)
      WRITE(6,102)(X2(J),J=1,JN)
101   FORMAT(25H0DISTANCES IN DIRECTION-1/(1H ,1P5E15.3))
102   FORMAT(25H0DISTANCES IN DIRECTION-2/(1H ,1P5E15.3))
      WRITE(6,101)(X1U(I),I=1,IN)
      WRITE(6,102)(X2U(J),J=1,JN)
      WRITE(6,103)
  103 FORMAT('0','THE DISTRIBUTION OF STREAM FUNCTION FROM PISTEP II
     1...NON-UNIFORM GRID'/)
      CALL PRINT(A,IN,JN)
      WRITE(6,104)
  104 FORMAT('0','THE DISTRIBUTION OF STREAMFUNCTION WITH A UNIFORM GRID
     1'/)
      CALL PRINT(AC,IN,JN)
      DO 300 I=1,IN
      DO 300 J=1,JN
      II=IN-I+1
      AM(I,J)=AC(J,II)
  300 CONTINUE
      WRITE(6,105) XRD,FAR
  105 FORMAT('0',T20,'XRD=',F8.4,5X,'FAR=',F8.4/)
      CALL CONTUR(AM,20,20,20,CL,-15,PTITLE,8,2,LTG)
      STOP
      END


      SUBROUTINE PRINT  (A,IN,JN)
      DIMENSION A(20,20)
      IA=IN/11
      DO 12 IB=1,IA
      IC=(IB-1)*11 +1
      ID=IB*11
      DO 5 L=1,JN
      J=JN-L+1
      WRITE(6,101) J,(A(I,J),I=IC,ID)
5     CONTINUE
      WRITE(6,103) (I,I=IC,ID)
      IF(ID.EQ.IN) GO TO 11
      IF(JN.GT.21) WRITE(6,105)
12    CONTINUE
      IE=ID+1
      DO 20 L=1,JN
      J=JN-L+1
```

```
      WRITE(6,111)  J,(A(I,J),I=IE,IN)
20    CONTINUE
      WRITE(6,113)(I,I=IE,IN)
11    CONTINUE
101   FORMAT(1H  I2,5X,1P11E11.3)
103   FORMAT(1HO,3X,11(9X,I2)//)
104   FORMAT(1H045X,28HCONTINUED IN THE I-DIRECTION//)
105   FORMAT(1H145X,28HCONTINUED IN THE I-DIRECTION//)
111   FORMAT(1H  I2,5X,1P10E11.3)
113   FORMAT(1HO,3X,10(9X,I2))
      RETURN
      END
C     ------------------------------------------------------------------
CCCCC
CCCCC     SUBROUTINE SPLIN
CCCCC
CCCCC     PURPOSE
CCCCC         PROVIDES INTERPOLATED VALUE USING "CUBIC SPLINE FITTING"
CCCCC
CCCCC     USAGE
CCCCC         FIRST CALL TO SUBROUTINE:
CCCCC         CALL SPLIN1(X,Y,M,XINT,YINT)
CCCCC
CCCCC         SUBSEQUENT CALLS:
CCCCC         CALL SPLINN(X,Y,M,XINT,YINT)
CCCCC
CCCCC     DESCRIPTION OF PARAMETERS
CCCCC         X:      MONOTONICALLY INCREASING ABSCISSA ARRAY
CCCCC         Y:      ONE-FOR-ONE CORRESPONDING ORDINATE ARRAY
CCCCC         M:      NUMBER OF X AND Y VALUES SUPPLIED < OR = 400
CCCCC         XINT:   VALUE OF ABSCISSA FOR WHICH CORRESPONDING ORDINATE
CCCCC                 IS TO BE INTERPOLATED (OR EXTRAPOLATED)
CCCCC         YINT:   INTERPOLATED (OR EXTRAPOLATED) ORDINATE VALUE
CCCCC
CCCCC         X,Y,XINT, AND YINT ARE REAL*8
CCCCC
CCCCC     REMARKS
CCCCC         IF SPECIFIED X FALLS OUTSIDE OF RANGE, AN EXTRAPOLATED
CCCCC         VALUE WILL BE SUPPLIED
CCCCC
CCCCC     SUBROUTINES AND FUNCTION SUBPROGRAMS REQUIRED
CCCCC         SUBROUTINE SPLICO IS INCLUDED IN SUBROUTINE SPLIN PACKAGE
CCCCC
CCCCC     MATHEMATICAL METHOD
CCCCC         UPON FIRST ENTRY TO SPLIN, A CALL TO SPLICO IS MADE TO
CCCCC         DETERMINE THE COEFFICIENTS TO BE USED IN PERFORMING THE
CCCC          INTERPOLATIONS. SEARCH FOR BRACKETING ABSCISSA VALUES IS
C             ALWAYS MADE FROM THE REFERENCE LAST USED IN INTERPOLATING.
```

```
C
C         REFERENCE
C            PENNINGTON, RALPH H.,"INTRODUCTORY COMPUTER METHODS AND
C            NUMERICAL ANALYSIS", THE MACMILLAN COMPANY, NEW YORK, 1965
C
C         SAMPLE PROGRAMS
C
C         1.   GIVEN 10 PAIRS OF ABSCISSA AND ORDINATE VALUES:
C
C              X=1.,5.,15.,21.,25.,32.,38.,44.,75.,90.
C              Y=0.,50.,250.,400.,750.,780.,900.,950.,975.,1100.
C
C              FIND AN ORDINATE VALUE WHEN THE ABSCISSA VALUE IS:
C              20.,60., AND 100.
C
C              REAL*8 X(10),Y(10),XINT(3)/20.,60.,100./,YINT(3)
C              CALL SPLIN1(X,Y,10,XINT(1),YINT(1))
C              DO 20 I=2,3
C          20  CALL SPLINN(X,Y,10,XINT(I),YINT(I))
C
C         2.   GIVEN A TWO DIMENSIONAL TABLE WITH N ROWS AND M COLUMNS,
C              N ABSCISSA VALUES, AND M ORDINATE VALUES, DETERMINE A
C              VALUE IN THE TABLE AT A SPECIFIED ABSCISSA AND ORDINATE
C              VALUE.
C
C              REAL*8 A(10,20),U(10),V(20),YY(20),YI(10),X,Y,FXY
C              N=10
C              M=20
C              DO 100 NR=1,N
C              DO 101 NC=1,M
C         101  YY(NC)=A(NR,NC)
C         100  CALL SPLIN1(V,YY,M,Y,YI(NR))
C              CALL SPLIN1(U,YI,N,X,FXY)
C
C              WHERE A CONTAINS THE TWO DIMENSIONAL TABLE
C                    N IS THE NUMBER OF ROWS IN A
C                    M IS THE NUMBER OF COLUMNS IN A
C                    U CONTAINS THE N ABSCISSA VALUES
C                    V CONTAINS THE M ORDINATE VALUES
C                    YY CONTAINS A SELECTED ROW OF THE TABLE A
C                    YI CONTAINS AN INTERPOLATED VALUE OF A FOR EACH ROW
C                       AT THE SELECTED ORDINATE VALUE
C                    X IS THE ABSCISSA FOR WHICH A FUNCTION VALUE
C                      IS INTERPOLATED
C                    Y IS THE ORDINATE FOR WHICH A FUNCTION VALUE IS
C                      TO BE RETURNED
C                    FXY IS A VALUE OF A AT X,Y
C
```

```
C
C
C
C     ------------------------------------------------------------------

      SUBROUTINE SPLIN1(X,Y,M,XINT,YINT)
      IMPLICIT REAL*8 (A-H),REAL*8 (O-Z)
      DIMENSION X(M),Y(M),C(4,400)
      CALL SPLICO(X,Y,M,C)
      K=1
      ENTRY SPLINN(X,Y,M,XINT,YINT)
    3 IF(XINT-X(1)) 70,1,2
   70 K=1
      GO TO 7
    1 YINT=Y(1)
      RETURN
    2 IF(XINT-X(K+1))6,4,5
    4 YINT=Y(K+1)
      RETURN
    5 K=K+1
      IF(M-K) 71,71,3
   71 K=M-1
      GO TO 7
    6 IF(XINT-X(K))13,12,11
   12 YINT=Y(K)
      RETURN
   13 K=K-1
      GO TO 6
    7 PRINT 101,XINT
  101 FORMAT(8HOXINT = E18.9,32H, OUT OF RANGE FOR INTERPOLATION)
   11 YINT=(X(K+1)-XINT)*(C(1,K)*(X(K+1)-XINT)**2+C(3,K))
      YINT=YINT+(XINT-X(K))*(C(2,K)*(XINT-X(K))**2+C(4,K))
      RETURN
      END


      SUBROUTINE SPLICO(X,Y,M,C)
      IMPLICIT REAL*8 (A-H),REAL*8 (O-Z)
      DIMENSION X(M),Y(M),C(4,400),D(400),P(400),E(400),A(400,3),B(400),
     1Z(400)
      MM=M-1
      DO 2 K=1,MM
      D(K)=X(K+1)-X(K)
      P(K)=D(K)/6.
    2 E(K)=(Y(K+1)-Y(K))/D(K)
      DO 3 K=2,MM
```

```
3 B(K)=E(K)-E(K-1)
  A(1,2)=-1.-D(1)/D(2)
  A(1,3)=D(1)/D(2)
  A(2,3)=P(2)-P(1)*A(1,3)
  A(2,2)=2.*(P(1)+P(2))-P(1)*A(1,2)
  A(2,3)=A(2,3)/A(2,2)
  B(2)=B(2)/A(2,2)
  DO 4 K=3,MM
  A(K,2)=2.*(P(K-1)+P(K))-P(K-1)*A(K-1,3)
  B(K)=B(K)-P(K-1)*B(K-1)
  A(K,3)=P(K)/A(K,2)
4 B(K)=B(K)/A(K,2)
  Q=D(M-2)/D(M-1)
  A(M,1)=1.+Q+A(M-2,3)
  A(M,2)=-Q-A(M,1)*A(M-1,3)
  B(M)=B(M-2)-A(M,1)*B(M-1)
  Z(M)=B(M)/A(M,2)
  MN=M-2
  DO 6 I=1,MN
  K=M-I
6 Z(K)=B(K)-A(K,3)*Z(K+1)
  Z(1)=-A(1,2)*Z(2)-A(1,3)*Z(3)
  DO 7 K=1,MM
  Q=1./(6.*D(K))
  C(1,K)=Z(K)*Q
  C(2,K)=Z(K+1)*Q
  C(3,K)=Y(K)/D(K)-Z(K)*P(K)
7 C(4,K)=Y(K+1)/D(K)-Z(K+1)*P(K)
  RETURN
  END
```

APPENDIX B: RAMJET DATA REDUCTION

```
C     COMPUTER PROGRAM TO REDUCE DATA FROM SOLID FUEL RAMJET RUNS
C     BY L. D. BOAZ
C     THE PARAMETERS IN THE PROGRAM ARE:
C        AF....AIR FUEL RATIO ON A MASS BASIS
C        AK....ASME FLOW COEFFICIENT
C        AS....NOZZLE THROAT AREA
C        BP....BAROMETRIC PRESSURE
C        CC*EQN..EMPIRICAL REGRESSION RATE EQUATION
C        D.....ORIFICE DIAMETER
C        DD....ORIFICE FLOW METER LARGE DIAMETER
C        DEF...FINAL EXIT DIAMETER
C        DEI...INITIAL EXIT DIAMETER
C        DP....ORIFICE DELTA P
C        DPC...DELTA CHAMBER PRESSURE (NOISE)
C        DPMM..DENSITY OF PMM, GM/IN**3
C        DS....NOZZLE THROAT DIAMETER
C        DSTEP.DIAMETER OF THE STEP HOLE
C        ERR...PERCENT ERROR BETWEEN RWT AND EMPIRICAL EQUATION
C        FG....GROSS THRUST
C        FISP..SPECIFIC IMPULSE
C        GAIR..MASS FLUX OF AIR
C        GL....GRAIN LENGTH
C        GM....RATIO OF SPECIFIC HEATS
C        GN....GRAIN NUMBER
C        H.....STEP HEIGHT
C        HD....STEP HEIGHT DEVIDED BY DIAMETER
C        NTOT.TOTAL NUMBER OF DATA POINTS TO READ IN
C        P.....ORIFICE PRESSURE
C        PC....CHAMBER PRESSURE
C        R.....GAS CONSTANT
C        RDE...REGRESSION RATE BASED ON EXIT DIAMETER
C        RED...REYNOLDS NUMBER BASED ON ORIFICE DIAMETER
C        RESTEP.STEP REYNOLDS NUMBER
C        RT....TOTAL RUN TIME WITH AIR
C        RWT...REGRESSION RATE BASED ON WEIGHT
C        SFC...SPECIFIC FUEL CONSUMPTION
C        T.....ORIFICE TEMPERATURE
C        TC....CHAMBER TEMPERATURE
C        TIG...TOTAL IGNITION TIME WITH METHANE
C        TIGA..IGNITION TIME INTO RUN
C        TIN...INLET TEMPERATURE
C        TM....TOTAL METHANE-OX (ONLY) TIME, INCLUDING MISFIRES
C        UPORT.MEAN CHAMBER VELOCITY
C        VIS...VISCOSITY
C        WDOT..WEIGHT FLOW RATE OF AIR
```

```
C         WF....WEIGHT FLOW RATE OF FUEL
C         WTF...FINAL GRAIN WEIGHT
C         WTI...INITIAL GRAIN WEIGHT
C         XR....FLOW REATTACHMENT POINT
C         XRD...XR DEVIDED BY DIAMETER
      INTEGER TEST,GN
      DIMENSION HD(30),XRD(30),SFC(30),EQN(30),C(30),ERR(30)
      DIMENSION AF(30),AMI(30),GAIR(30),DSTEP(30),UPORT(30)
      DIMENSION TEST(30),T(30),P(30),DP(30),BP(30),TIN(30),RT(30),
     1TIG(30),TIGA(30),PC(30),XR(30),DPC(30),H(30),DS(30),GN(30),
     2WTI(30),WTF(30),DEI(30),DEF(30),GL(30)
      DIMENSION WDOT(30),AK(30),RESTEP(30),TC(30),RWT(30),RDE(30),
     1WF(30),FG(30),FISP(30),D(30),TM(30)
C     THE FOLLOWING PARAMETERS ARE USED WITH THE SUBROUTINE SPLIN
C     TO INTERPOLATE TABULATED VALUES OF ASME FLOW COEFFICIENT.
      REAL*8 A(10,7),U(10),V(7),YY(7),YI(10),X,Y,FXY
      DO 501 I=1,10
      READ(5,502) U(I),A(I,1),A(I,2),A(I,3),A(I,4),A(I,5),A(I,6),A(I,7)
  502 FORMAT(D10.3,7D10.4)
  501 CONTINUE
      DO 504 I=1,7
      READ(5,505) V(I)
  505 FORMAT(D15.0)
  504 CONTINUE
      NTOT=29
      DO 100 N=1,NTOT
      READ(5,510) TEST(N),GN(N),T(N),P(N),DP(N),BP(N),TIN(N),RT(N)
  510 FORMAT(2I10,6F10.5)
      READ(5,511) TIG(N),TIGA(N),PC(N),XR(N),DPC(N),H(N),DS(N),WTI(N)
  511 FORMAT(8F10.5)
      READ(5,512) WTF(N),DEI(N),DEF(N),GL(N),DSTEP(N),D(N),TM(N)
  512 FORMAT(7F10.5)
  100 CONTINUE
      WRITE(6,600)
  600 FORMAT('1',////////,T44,'SOLID FUEL RAMJET DATA REDUCTION')
      WRITE(6,605)
  605 FORMAT('0',T21,'INPUT DATA'/)
      WRITE(6,610)
  610 FORMAT('0',T21,'TEST#',T28,'GRAIN#',T36,'ORIFICE',T45,'ORIFICE',
     1T54,'DELTA-P',T63,'BAROMETRIC',T75,'INLET',T82,'RUN TIME',
     2T92,'IGNITION'/T37,'T (F)',T45,'P (PSIG)',T55,'(PSI) ',T63,'P (IN.
     3HG.)',T75,'T (F)',T83,'(SEC)',T94,'TIME'//)
      DO 200 N=1,NTOT
  200 WRITE(6,620) TEST(N),GN(N),T(N),P(N),DP(N),BP(N),TIN(N),RT(N),
     1TIG(N)
  620 FORMAT(' ',T22,I2,T30,I2,T37,F5.1,T46,F5.1,T55,F5.2,T64,F5.2,
     1T75,F5.1,T84,F5.2,T94,F4.2)
      WRITE(6,606)
```

```
  606 FORMAT('1',////////,T21,'INPUT DATA'/)
      WRITE(6,611)
  611 FORMAT('0',T21,'TEST#',T28,'IG.TIME',T37,'REAT.PT.',T47,'CHAMBER'
     1,T56,'PC NOISE',T66,'NOZZLE',T74,'INITIAL',T84,'FINAL',T92,'STEP H
     2'/T27,'INTO RUN',T39,'(IN)',T47,'P (PSIG)',T57,'(PSIA)',T66,'D* (I
     3N)',T74,'WT (GM)',T83,'WT (GM)',T93,'(IN)'//)
      DO 240 N=1,NTOT
  240 WRITE(6,621) TEST(N),TIGA(N),XR(N),PC(N),DPC(N),DS(N),WTI(N),
     1WTF(N),H(N)
  621 FORMAT(' ',T22,I2,T29,F5.3,T39,F4.2,T48,F5.1,T58,F5.2,T66,F5.3,T74
     1,F6.1,T83,F6.1,T93,F5.3)
      WRITE(6,606)
      WRITE(6,612)
  612 FORMAT('0',T21,'TEST#',T28,'INITIAL',T37,'FINAL',T44,'GR.LENGTH',
     1T55,'DSTEP',T65,'TM'/T28,'D (IN)',T37,'D (IN)',T46,'(IN)',T56,
     2'(IN)',T63,'(SEC)'//)
      DO 245 N=1,NTOT
  245 WRITE(6,622) TEST(N),DEI(N),DEF(N),GL(N),DSTEP(N),TM(N)
  622 FORMAT(' ',T22,I2,T28,F5.3,T37,F5.3,T45,F6.3,T55,F5.3,T63,F5.2)
      DO=2.46
      DO 210 N=1,NTOT
      BP(N)=BP(N)*0.491157
      P(N)=P(N)+BP(N)
      PC(N)=PC(N)+BP(N)
      T(N)=T(N)+459.67
      TIN(N)=TIN(N)+459.67
      VIS=.00001241*(T(N)/540.0)**0.72253
C     CALCULATE REYNOLDS NUMBER BY GUESSING THE FLOW RATE.
      WDOT(N)=.25
      RED=6.210925*WDOT(N)/VIS
      BETA=D(N)/DO
      X=DBLE(BETA)
      Y=DBLE(RED)
      NN=10
      M=7
      DO 110 NR=1,NN
      DO 111 NC=1,M
  111 YY(NC)=A(NR,NC)
  110 CALL SPLIN1(V,YY,M,Y,YI(NR))
      CALL SPLIN1(U,YI,NN,X,FXY)
      CK=SNGL(FXY)
      YF=1.0-(0.41+(0.35*(BETA**4.0)))*DP(N)/(1.4*P(N))
      WDOT(N)=0.86234829*CK*D(N)*D(N)*YF*SQRT(DP(N)*P(N)/T(N))
C     RECALCULATE RED AND WDOT
      RED=6.210925*WDOT(N)/VIS
      Y=DBLE(RED)
      DO 120 NR=1,NN
      DO 121 NC=1,M
```

```
121 YY(NC)=A(NR,NC)
120 CALL SPLIN1(V,YY,M,Y,YI(NR))
    CALL SPLIN1(U,YI,NN,X,FXY)
    CK=SNGL(FXY)
    AK(N)=CK
    WDOT(N)=0.86234829*CK*D(N)*D(N)*YF*SQRT(DP(N)*P(N)/T(N))
    AS=3.14159*DS(N)*DS(N)/4.0
    GM=1.1
    R=50.0
    WTI(N)=WTI(N)-3.2*TM(N)
    WF(N)=((WTI(N)-WTF(N))/RT(N))/453.59237
    TC(N)=((AS*PC(N)/(WDOT(N)+WF(N)))**2.0)*(GM*32.174/R)*((2.0/(GM+1.
   10))**((GM+1.0)/(GM-1.0)))
    RDE(N)=(DEF(N)-DEI(N))/(2.0*RT(N))
    DPMM=19.6405
    RWT(N)=(SQRT((4.0*(WTI(N)-WTF(N))/(DPMM*GL(N)*3.14159))+(DEI(N)*
   1DEI(N)))-DEI(N))/(2.0*RT(N))
    GC=32.174
    FG(N)=(WF(N)+WDOT(N))*SQRT((2.0*GC*GM*R*TC(N)/(GM-1.0))*(1.0-
   1((BP(N)/PC(N))**((GM-1.0)/GM))))/GC
    FISP(N)=FG(N)/WF(N)
    VIS=.00001241*(TIN(N)/540.0)**0.72253
    RESTEP(N)=48.*WDOT(N)*H(N)/(VIS*3.14159*2.25)
    ASTEP=3.14159*DSTEP(N)*DSTEP(N)/4.0
    AF(N)=WDOT(N)/WF(N)
    AAVE=3.14159*DEI(N)*DEI(N)/4.0
    GAIR(N)=WDOT(N)/AAVE
    UPORT(N)=WDOT(N)*R*TC(N)/(PC(N)*AAVE)
    HD(N)=H(N)/DEI(N)
    XRD(N)=XR(N)/DEI(N)
    SFC(N)=3600.*WF(N)/FG(N)
    EQN(N)=(PC(N)**0.51)*(TIN(N)**0.34)*(GAIR(N)**0.41)
    C(N)=RWT(N)/EQN(N)
210 CONTINUE
    WRITE(6,607)
607 FORMAT('1',////////,T21,'CALCULATED RESULTS'/)
    WRITE(6,613)
613 FORMAT('0',T21,'TEST#',T29,'WDOT',T37,'CHAMBER',T46,'CHAMBER',
   1T58,'RWT',T68,'RDE',T79,'WF',T87,'RESTEP',T96,'FG'/T27,'(LBM/SEC)'
   2,T38,'T (R)',T46,'P (PSIA)',T56,'(IN/SEC)',T66,'(IN/SEC)',T77,
   3'(LBM/SEC)',T95,'(LBF)'//)
    DO 270 N=1,NTOT
270 WRITE(6,623) TEST(N),WDOT(N),TC(N),PC(N),RWT(N),RDE(N),WF(N),
   1RESTEP(N),FG(N)
623 FORMAT(' ',T22,I2,T29,F5.3,T37,F6.1,T48,F5.1,T57,F6.4,T67,F6.4,
   2T78,F6.4,T86,F7.0,T97,F3.0)
    WRITE(6,607)
    WRITE(6,614)
```

```
614 FORMAT('0',T21,'TEST#',T29,'AF',T37,'GAIR',T46,'H/D',T54,
   1'XR/D',T64,'UPORT',T74,'ISP',T83,'SFC'/T32,'(LBM/SEC.IN2)',T62,
   2'(FT/SEC)',T73,'(SEC)'//)
    DO 280 N=1,NTOT
280 WRITE(6,624) TEST(N),AF(N),GAIR(N),HD(N),XRD(N),UPORT(N),
   1FISP(N),SFC(N)
624 FORMAT(' ',T22,I2,T27,F5.2,T36,F5.3,T45,F5.3,T54,F4.2,
   1T64,F4.0,T73,F5.0,T83,F3.1)
    DO 750 N=1,NTOT
    CC=0.00023
    IF(HD(N).GT.0.4) CC=0.00034
    EQN(N)=CC*EQN(N)
750 ERR(N)=ABS((EQN(N)-RWT(N))/RWT(N))*100.0
    WRITE(6,607)
    WRITE(6,615)
615 FORMAT('0',T21,'TEST',T27,'EMPIRICAL',T40,'RWT',T47,'PERCENT'/
   1T28,'EQUATION',T38,'(IN/SEC)',T48,'ERROR'//)
    DO 290 N=1,NTOT
290 WRITE(6,625) TEST(N),EQN(N),RWT(N),ERR(N)
625 FORMAT(' ',T22,I2,T28,F7.5,T38,F7.5,T48,F4.1)
    WRITE(6,760)
760 FORMAT('1',T30,'RWT VS. C*EQN'//)
    CALL PLOTP(EQN,RWT,-NTOT,0)
    STOP
    END
```

SOLID FUEL RAMJET DATA REDUCTION

INPUT DATA

TEST#	GRAIN#	ORIFICE T (F)	ORIFICE P (PSIG)	DELTA-P (PSI)	BAROMETRIC P (IN.HG.)	INLET T (F)	RUN TIME (SEC)	IGNITION TIME
6	2	70.0	128.0	3.70	29.67	71.0	30.23	3.91
7	3	70.0	70.0	2.00	29.67	70.0	30.15	3.99
8	4	70.0	135.0	3.50	29.67	71.0	30.19	3.36
10	5	70.0	129.0	3.20	29.67	71.0	30.18	5.32
15	7	65.0	126.5	18.80	29.86	66.0	30.37	4.02
18	8	65.0	128.0	17.00	29.86	65.0	30.32	5.63
19	9	207.0	127.5	4.80	29.79	191.0	30.13	3.56
20	10	212.0	128.0	4.20	29.79	195.0	30.23	3.79
21	11	215.0	134.0	3.75	29.79	197.0	30.41	4.44
32	15	210.0	125.0	14.80	29.80	199.0	31.76	4.41
39	17	354.0	125.5	4.80	29.78	345.0	30.35	4.38
42	18	360.0	126.5	4.80	29.78	348.0	30.57	7.37
48	20	375.0	126.0	4.80	29.78	362.0	30.25	3.48
49	21	370.0	122.0	4.80	29.78	354.0	30.32	3.41
52	13	385.0	123.0	7.50	29.78	365.0	24.28	5.40
53	16	387.0	119.0	16.00	29.78	371.0	30.57	4.75
58	2	220.0	123.0	4.00	28.90	202.0	30.41	4.00
60	22	223.0	127.0	4.25	28.90	203.0	30.54	7.06
61	23	222.0	134.0	3.75	29.89	205.0	30.22	3.67
62	24	212.0	140.0	4.60	29.89	195.0	30.39	4.65
63	25	203.0	138.5	8.20	29.89	191.0	30.16	3.48
66	27	202.0	135.0	5.80	29.89	190.0	30.44	4.46
67	28	200.0	128.0	4.40	29.89	187.0	30.50	4.16
69	29	66.0	134.0	4.75	30.09	63.0	30.43	5.23
70	30	67.0	128.0	3.70	30.09	65.0	30.46	6.88
71	31	70.0	129.0	3.30	30.09	67.0	30.62	4.93
72	32	341.0	138.0	5.00	30.08	335.0	30.33	5.25
73	33	329.0	137.0	6.25	30.08	325.0	30.29	4.39
74	34	325.0	128.0	5.80	30.08	320.0	30.44	4.44

INPUT DATA

TEST#	IG.TIME INTO RUN	REAT.PT. (IN)	CHAMBER P (PSIG)	PC NOISE (PSIA)	NOZZLE D* (IN)	INITIAL WT (GM)	FINAL WT (GM)	STEP H (IN)
6	1.560	3.00	45.0	6.00	0.747	2570.0	2306.5	0.500
7	1.720	3.20	37.5	16.00	0.632	2641.0	2444.0	0.500
8	1.560	2.45	71.5	24.00	0.632	2612.0	2329.5	0.500
10	2.110	2.58	87.0	30.00	0.583	2585.0	2242.0	0.500
15	1.910	3.07	47.0	5.00	0.995	2636.0	2239.0	0.500
18	1.940	2.82	69.0	6.00	0.877	2626.5	2196.0	0.500
19	0.877	3.14	49.0	5.00	0.747	2688.0	2402.5	0.500
20	1.350	2.81	74.0	26.00	0.632	2590.0	2284.5	0.500
21	1.260	2.72	88.0	27.00	0.583	2509.5	2182.5	0.500
32	0.917	2.00	59.5	3.00	0.877	2623.0	2172.0	0.500
39	0.563	2.65	75.0	23.00	0.632	2736.5	2377.0	0.500
42	1.300	2.61	76.0	24.00	0.632	2734.5	2346.5	0.500
48	0.790	2.57	92.5	26.00	0.583	2648.0	2208.0	0.500
49	0.940	2.45	89.0	26.00	0.583	2732.0	2373.5	0.500
52	0.830	2.91	108.0	12.00	0.583	2542.0	2181.0	0.500
53	0.850	3.00	86.0	5.00	0.747	2717.5	2207.5	0.500
58	0.690	4.05	41.0	4.00	0.583	1200.0	1056.0	0.625
60	1.110	3.75	56.5	2.50	0.583	2734.0	2288.5	0.625
61	0.650	4.00	84.0	3.00	0.475	2670.0	2293.0	0.625
62	1.270	3.70	42.0	2.00	0.674	2778.5	2403.0	0.625
63	0.550	2.88	53.0	15.00	0.674	2713.0	2450.0	0.500
66	0.880	2.57	82.0	29.00	0.540	2747.0	2398.5	0.500
67	0.630	2.32	91.0	26.00	0.475	2763.0	2477.0	0.500
69	1.770	2.42	41.0	15.00	0.674	2637.0	2393.0	0.500
70	2.020	2.32	72.0	26.00	0.540	2631.5	2331.0	0.500
71	1.460	2.30	92.5	30.00	0.475	2702.5	2357.0	0.500
72	1.180	2.53	96.5	24.00	0.475	2655.5	2289.5	0.500
73	1.160	2.34	81.0	21.00	0.540	2731.0	2394.5	0.500
74	1.000	2.63	40.5	5.00	0.674	2684.0	2450.0	0.500

INPUT DATA

TEST#	INITIAL D (IN)	FINAL D (IN)	GR.LENGTH (IN)	DSTEP (IN)	TM (SEC)
6	1.500	1.917	12.155	0.503	3.92
7	1.491	1.816	12.215	0.503	2.27
8	1.495	1.960	12.083	0.503	1.80
10	1.508	2.046	11.981	0.503	4.93
15	1.504	2.105	12.185	0.503	2.10
18	1.496	2.160	12.145	0.503	7.71
19	1.518	1.964	12.030	0.503	2.68
20	1.496	1.990	12.075	0.503	2.44
21	1.502	2.044	11.830	0.503	3.18
32	1.505	2.209	11.995	0.503	6.74
39	1.505	2.028	11.965	0.503	10.98
42	1.510	2.084	11.965	0.503	12.93
48	1.508	2.120	11.965	0.503	21.14
49	1.565	2.137	11.985	0.503	2.47
52	1.512	2.070	12.075	0.503	10.17
53	1.534	2.290	11.925	0.503	3.90
58	1.508	2.200	5.887	0.250	2.63
60	1.510	1.955	11.985	0.250	9.10
61	1.501	1.952	11.975	0.250	3.02
62	1.502	1.930	12.009	0.250	3.38
63	1.511	1.947	12.015	0.503	2.93
66	1.505	2.018	11.925	0.503	6.74
67	1.508	1.988	11.975	0.503	3.53
69	1.514	1.910	12.015	0.503	6.59
70	1.505	1.956	11.956	0.503	4.86
71	1.495	1.976	11.998	0.503	3.47
72	1.500	2.017	11.920	0.503	4.07
73	1.510	2.030	11.978	0.503	3.23
74	1.510	1.896	12.000	0.503	3.44

CALCULATED RESULTS

TEST#	WDOT (LBM/SEC)	CHAMBER T (R)	CHAMBER P (PSIA)	RWT (IN/SEC)	RDE (IN/SEC)	WF (LBM/SEC)	RESTEP	FG (LBF)
6	0.199	3657.3	59.6	0.0065	0.0069	0.0183	55220.	27.
7	0.113	4203.6	52.1	0.0051	0.0054	0.0139	31385.	16.
8	0.199	3865.5	86.1	0.0072	0.0077	0.0202	55052.	31.
10	0.186	4229.9	101.6	0.0083	0.0089	0.0239	51600.	32.
15	0.434	2734.9	61.7	0.0095	0.0099	0.0283	121021.	49.
18	0.417	3261.8	83.7	0.0099	0.0109	0.0295	116361.	57.
19	0.202	4012.2	63.6	0.0071	0.0074	0.0203	48218.	29.
20	0.189	4443.4	88.6	0.0077	0.0082	0.0217	44883.	32.
21	0.182	4552.5	102.6	0.0082	0.0089	0.0230	43161.	33.
32	0.342	3683.7	74.1	0.0100	0.0111	0.0298	81086.	49.
39	0.181	4783.6	89.6	0.0082	0.0086	0.0236	37193.	32.
42	0.181	4823.4	90.6	0.0087	0.0094	0.0250	37092.	33.
48	0.179	4871.2	107.1	0.0093	0.0101	0.0271	36240.	34.
49	0.177	4727.4	103.6	0.0086	0.0094	0.0255	36073.	33.
52	0.219	4395.2	122.6	0.0103	0.0115	0.0298	44137.	40.
53	0.308	4167.5	100.6	0.0117	0.0124	0.0359	61824.	52.
58	0.116	3472.0	55.2	0.0071	0.0114	0.0098	34316.	15.
60	0.121	3954.7	70.7	0.0101	0.0073	0.0301	35752.	20.
61	0.117	3752.1	98.7	0.0092	0.0075	0.0268	34466.	21.
62	0.133	4084.9	56.7	0.0091	0.0070	0.0265	39587.	20.
63	0.177	3892.4	67.7	0.0066	0.0072	0.0185	42217.	26.
66	0.148	4245.6	96.7	0.0083	0.0084	0.0237	35335.	26.
67	0.126	4184.7	105.7	0.0071	0.0079	0.0199	30279.	22.
69	0.150	3660.7	55.8	0.0058	0.0065	0.0161	41919.	20.
70	0.130	4450.4	86.8	0.0073	0.0074	0.0206	36187.	23.
71	0.123	4271.0	107.3	0.0084	0.0079	0.0241	34139.	23.
72	0.126	4283.6	111.3	0.0089	0.0085	0.0257	26118.	24.
73	0.141	4488.0	95.8	0.0083	0.0086	0.0237	29510.	26.
74	0.132	4477.9	55.3	0.0059	0.0063	0.0162	27780.	20.

CALCULATED RESULTS

TEST#	AF	GAIR (LBM/SEC.IN2)	H/D	XR/D	UPORT (FT/SEC)	ISP (SEC)	SFC
6	10.89	0.113	0.333	2.00	346.	1457.	2.5
7	8.15	0.065	0.335	2.15	262.	1147.	3.1
8	9.83	0.113	0.334	1.64	254.	1521.	2.4
10	7.79	0.104	0.332	1.71	217.	1345.	2.7
15	15.31	0.244	0.332	2.04	541.	1745.	2.1
18	14.12	0.237	0.334	1.89	462.	1931.	1.9
19	9.95	0.111	0.329	2.07	351.	1435.	2.5
20	8.68	0.107	0.334	1.88	269.	1467.	2.5
21	7.91	0.103	0.333	1.81	227.	1416.	2.5
32	11.48	0.192	0.332	1.33	478.	1640.	2.2
39	7.70	0.102	0.332	1.76	272.	1371.	2.6
42	7.25	0.101	0.331	1.73	269.	1310.	2.7
48	6.61	0.100	0.332	1.70	228.	1264.	2.8
49	6.96	0.092	0.319	1.57	210.	1291.	2.8
52	7.35	0.122	0.331	1.92	219.	1356.	2.7
53	8.60	0.167	0.326	1.96	346.	1453.	2.5
58	11.82	0.065	0.414	2.69	205.	1506.	2.4
60	4.03	0.068	0.414	2.48	189.	682.	5.3
61	4.37	0.066	0.416	2.66	126.	767.	4.7
62	5.03	0.075	0.416	2.46	271.	766.	4.7
63	9.52	0.098	0.331	1.90	283.	1383.	2.6
66	6.23	0.083	0.332	1.71	182.	1094.	3.3
67	6.35	0.071	0.332	1.54	140.	1127.	3.2
69	9.27	0.083	0.330	1.60	273.	1225.	2.9
70	6.28	0.073	0.332	1.54	187.	1095.	3.3
71	5.09	0.070	0.334	1.54	139.	945.	3.8
72	4.92	0.071	0.333	1.69	137.	928.	3.9
73	5.95	0.079	0.331	1.55	185.	1076.	3.3
74	8.20	0.074	0.331	1.74	299.	1210.	3.0

CALCULATED RESULTS

TEST	EMPIRICAL EQUATION	RWT (IN/SEC)	PERCENT ERROR
6	0.00638	0.00652	2.2
7	0.00474	0.00508	6.6
8	0.00771	0.00718	7.3
10	0.00811	0.00834	2.7
15	0.00889	0.00953	6.8
18	0.01025	0.00994	3.1
19	0.00704	0.00714	1.5
20	0.00822	0.00765	7.4
21	0.00871	0.00816	6.8
32	0.00956	0.01002	4.6
39	0.00869	0.00825	5.3
42	0.00872	0.00865	0.8
48	0.00952	0.00932	2.2
49	0.00901	0.00857	5.1
52	0.01106	0.01030	7.4
53	0.01140	0.01169	2.5
58	0.00780	0.00712	9.6
60	0.00900	0.01013	11.1
61	0.01059	0.00924	14.6
62	0.00836	0.00910	8.2
63	0.00690	0.00663	4.1
66	0.00771	0.00830	7.1
67	0.00754	0.00707	6.7
69	0.00542	0.00584	7.3
70	0.00644	0.00734	12.3
71	0.00706	0.00842	16.2
72	0.00835	0.00893	6.6
73	0.00802	0.00828	3.1
74	0.00589	0.00586	0.5

APPENDIX C: NON-SUSTAINING TEST DATA

```
C       COMPUTER PROGRAM TO REDUCE DATA FROM SOLID FUEL RAMJET RUNS
C       FOR NON-SUSTAINING TESTS.
C       BY L. D. BOAZ
        INTEGER TEST,GN
        DIMENSION D(40),WDOT(40),AK(40),RESTEP(40),HD(40)
        DIMENSION AM1(40),GAIR(40),DSTEP(40),UPORT(40),TEST(40),T(40),
       1P(40),DP(40),BP(40),TIN(40),PC(40),H(40)
        REAL*8 A(10,7),U(10),V(7),YY(7),YI(10),X,Y,FXY
        DATA DSTEP/3*.75,3*.503/
        DATA D/3*.626,5*.504/
        DO 501 I=1,10
        READ(5,502) U(I),A(I,1),A(I,2),A(I,3),A(I,4),A(I,5),A(I,6),A(I,7)
    502 FORMAT(D10.3,7D10.4)
    501 CONTINUE
        DO 504 I=1,7
        READ(5,505) V(I)
    505 FORMAT(D15.0)
    504 CONTINUE
        NTOT=36
        DO 100 N=1,NTOT
        READ(5,510) TEST(N),T(N),P(N),DP(N),BP(N),TIN(N),PC(N)
    510 FORMAT(I2,T10,6F10.5)
    100 CONTINUE
        WRITE(6,600)
    600 FORMAT('1',////////,T33,'SOLID FUEL RAMJET DATA REDUCTION, NON-SUS
       1TAINING TESTS')
        WRITE(6,605)
    605 FORMAT('0',T21,'INPUT DATA')
        WRITE(6,610)
    610 FORMAT('0',T21,'TEST',T30,'T',T38,'P',T45,'DP',T53,'BP',T62,'TIN',
       1T71,'PC',T78,'DSTEP',T85,'ORIFICE D',T98,'H'/T29,'(F)',T35,'(PSIG)
       2',T44,'(PSI)',T51,'(IN HG)',T62,'(F)',T69,'(PSIG)',T79,'(IN)',T87,
       3'(IN)',T96,'(IN)'//)
        DO 200 N=1,NTOT
        H(N)=(1.5-DSTEP(N))/2.0
    200 WRITE(6,620) TEST(N),T(N),P(N),DP(N),BP(N),TIN(N),PC(N),DSTEP(N),
       1D(N),H(N)
    620 FORMAT(' ',T22,I2,T29,F5.1,T36,F5.1,T44,F4.1,T52,F5.2,T61,F5.1,T70
       1,F4.1,T78,F5.3,T87,F5.3,T96,F5.3)
        DD=2.46
        DO 210 N=1,NTOT
        BP(N)=BP(N)*0.491157
        P(N)=P(N)+BP(N)
        PC(N)=PC(N)+BP(N)
        T(N)=T(N)+459.67
```

```
      TIN(N)=TIN(N)+459.67
      VIS=.00001241*(T(N)/540.0)**0.72253
      WDOT(N)=.25
      RED=6.210925*WDOT(N)/VIS
      BETA=D(N)/DD
      X=DBLE(BETA)
      Y=DBLE(RED)
      NN=10
      M=7
      DO 110 NR=1,NN
      DO 111 NC=1,M
  111 YY(NC)=A(NR,NC)
  110 CALL SPLIN1(V,YY,M,Y,YI(NR))
      CALL SPLIN1(U,YI,NN,X,FXY)
      CK=SNGL(FXY)
      YF=1.0-(0.41+(0.35*(BETA**4.0)))*DP(N)/(1.4*P(N))
      WDOT(N)=0.86234829*CK*D(N)*D(N)*YF*SQRT(DP(N)*P(N)/T(N))
      RED=6.210925*WDOT(N)/VIS
      Y=DBLE(RED)
      DO 120 NR=1,NN
      DO 121 NC=1,M
  121 YY(NC)=A(NR,NC)
  120 CALL SPLIN1(V,YY,M,Y,YI(NR))
      CALL SPLIN1(U,YI,NN,X,FXY)
      CK=SNGL(FXY)
      AK(N)=CK
      WDOT(N)=0.86234829*CK*D(N)*D(N)*YF*SQRT(DP(N)*P(N)/T(N))
      GM=1.4
      R=53.35
      ASTEP=3.14159*DSTEP(N)*DSTEP(N)/4.0
      AAVE=3.14159*1.5*1.5/4.0
      GAIR(N)=WDOT(N)/AAVE
      UPORT(N)=WDOT(N)*R*TIN(N)/(PC(N)*AAVE)
      VIS=.00001241*(TIN(N)/540.0)**0.72253
      RESTEP(N)=48.*WDOT(N)*H(N)/(VIS*3.14159*2.25)
      HD(N)=H(N)/1.5
  210 CONTINUE
      WRITE(6,625)
  625 FORMAT('1',////////,T21,'CALCULATED RESULTS'//)
      WRITE(6,630)
  630 FORMAT(' ',T21,'TEST',T30,'H/D',T40,'WDOT',T49,'RESTEP',T61,'GAIR'
     1,T72,'UPORT',T83,'  '/T38,'LBM/SEC)',T56,'(LBM/SEC-IN2)',T71,
     2'(FT/SEC)'//)
      DO 300 N=1,NTOT
  300 WRITE(6,640) TEST(N),HD(N),WDOT(N),RESTEP(N),GAIR(N),UPORT(N)
  640 FORMAT(' ',T22,I2,T29,F5.3,T39,F5.3,T49,F7.0,T61,F5.3,T72,F5.1)
      STOP
      END
```

SOLID FUEL RAMJET DATA REDUCTION, NON-SUSTAINING TESTS

INPUT DATA

TEST	T (F)	P (PSIG)	DP (PSI)	BP (IN HG)	TIN (F)	PC (PSIG)	DSTEP (IN)	ORIFICE D (IN)	H (IN)
1	70.0	130.0	4.0	29.67	70.0	9.0	0.750	0.626	0.375
2	70.0	132.0	4.0	29.67	70.0	10.0	0.750	0.626	0.375
3	70.0	134.0	4.0	29.67	70.0	27.0	0.750	0.626	0.375
5	70.0	137.0	4.0	29.67	71.0	15.0	0.503	0.626	0.498
9	70.0	134.0	5.0	29.67	71.0	30.0	0.503	0.626	0.498
11	65.0	126.0	16.0	29.86	63.0	5.0	0.503	0.626	0.498
12	65.0	128.0	19.5	29.86	62.0	5.0	0.503	0.626	0.498
16	65.0	126.0	19.0	29.86	65.0	20.0	0.503	0.626	0.498
17	65.0	126.0	18.3	29.86	65.0	20.0	0.503	0.626	0.498
22	213.0	125.0	20.0	29.80	203.0	3.0	0.503	0.626	0.498
23	212.0	125.0	20.0	29.80	200.0	4.0	0.503	0.626	0.498
24	212.0	127.5	20.4	29.80	200.0	4.0	0.503	0.626	0.498
25	209.0	127.0	20.2	29.80	198.0	4.0	0.503	0.626	0.498
26	207.0	125.0	20.0	29.80	196.0	13.5	0.503	0.626	0.498
27	208.0	125.0	20.0	29.80	196.0	13.0	0.503	0.626	0.498
28	209.0	125.5	18.5	29.80	196.0	13.0	0.503	0.626	0.498
29	209.0	127.5	18.7	29.80	197.0	13.0	0.503	0.626	0.498
30	209.0	125.0	18.2	29.80	200.0	13.0	0.503	0.626	0.498
31	210.0	125.0	18.2	29.80	200.0	21.0	0.503	0.626	0.498
33	218.0	133.0	17.8	29.80	207.0	13.0	0.503	0.626	0.498
34	212.0	73.0	10.5	29.80	198.0	3.0	0.503	0.626	0.498
35	211.0	73.0	10.5	29.80	198.0	4.0	0.503	0.626	0.498
36	213.0	128.0	17.0	29.80	202.0	7.5	0.503	0.626	0.498
37	360.0	123.5	6.0	29.78	350.0	15.0	0.503	0.626	0.498
38	356.0	123.0	6.0	29.78	347.0	14.0	0.503	0.626	0.498
40	358.0	125.0	6.0	29.78	348.0	26.0	0.503	0.626	0.498
41	356.0	125.0	6.5	29.78	347.0	27.0	0.503	0.626	0.498
46	360.0	122.0	8.0	29.78	347.0	37.0	0.503	0.626	0.498
47	366.0	122.0	8.0	29.78	355.0	40.0	0.503	0.626	0.498
50	370.0	120.0	8.5	29.78	355.0	16.0	0.503	0.626	0.498
51	372.0	125.0	8.5	29.78	362.0	16.0	0.503	0.626	0.498
54	226.0	128.0	20.0	28.96	212.0	30.0	0.503	0.504	0.498
55	227.0	128.0	20.0	28.96	212.0	30.0	0.503	0.504	0.498
56	230.0	130.0	20.0	28.96	214.0	37.0	0.503	0.504	0.498
57	230.0	131.0	20.5	28.96	215.0	38.0	0.503	0.504	0.498
65	202.0	128.0	7.0	29.87	178.0	21.0	0.503	0.504	0.498

CALCULATED RESULTS

TEST	H/D	WDOT (LBM/SEC)	RESTEP	GAIR (LBM/SEC-IN2)	UPORT (FT/SEC)
1	0.250	0.209	43394.	0.118	141.5
2	0.250	0.210	43697.	0.119	136.7
3	0.250	0.211	43998.	0.120	81.3
5	0.332	0.214	59002.	0.121	115.7
9	0.332	0.236	65149.	0.133	84.8
11	0.332	0.402	112261.	0.227	322.5
12	0.332	0.444	124078.	0.251	355.3
16	0.332	0.435	121178.	0.246	198.8
17	0.332	0.428	119112.	0.242	195.4
22	0.332	0.392	92263.	0.222	444.8
23	0.332	0.392	92635.	0.222	419.4
24	0.332	0.400	94376.	0.226	427.3
25	0.332	0.398	94190.	0.225	424.2
26	0.332	0.394	93388.	0.223	277.1
27	0.332	0.394	93319.	0.223	281.9
28	0.332	0.380	90164.	0.215	272.4
29	0.332	0.385	91203.	0.218	276.3
30	0.332	0.377	88927.	0.213	271.5
31	0.332	0.376	88861.	0.213	210.4
33	0.332	0.382	89409.	0.216	278.0
34	0.332	0.227	53767.	0.129	255.9
35	0.332	0.227	53807.	0.129	242.3
36	0.332	0.368	86718.	0.208	332.2
37	0.332	0.200	40704.	0.113	165.0
38	0.332	0.200	40837.	0.113	170.2
40	0.332	0.201	41053.	0.114	120.8
41	0.332	0.210	42769.	0.119	122.6
46	0.332	0.229	46642.	0.129	107.8
47	0.332	0.228	46143.	0.129	102.5
50	0.332	0.232	47033.	0.131	186.4
51	0.332	0.236	47576.	0.134	191.3
54	0.332	0.254	59226.	0.144	116.6
55	0.332	0.254	59183.	0.144	116.5
56	0.332	0.255	59375.	0.145	101.4
57	0.332	0.259	60208.	0.147	101.1
65	0.332	0.158	38173.	0.089	85.2

LIST OF REFERENCES

1. Abbott, D. E. and Kline, J. S., "Experimental Investigation of Subsonic Turbulent Flow Over Single and Double Backward Facing Steps," Journal of Basic Engineering, p. 317, September 1962.

2. Krall, K. M. and Sparrow, E. M., "Turbulent Heat Transfer in the Separated, Reattached, and Redevelopment Regions of a Circular Tube," Journal of Heat Transfer, p.131, February 1966.

3. Netzer, D. W., Hybrid Rocket Internal Ballistics, Naval Postgraduate School, CPIA Publication No. 222. January 1972.

4. Muzzy, R. J., "Applied Hybrid Combustion Theory," A.I.A.A. Paper 72-1143, December 1972.

5. United Technology Center, Sunnyvale, California, Investigation of Fundamental Phenomena in Hybrid Propulsion (U), Vol. I (U), Final Technical Report No. UTC 2097-FR, Contract No. w 64-0659-c, November 1965.

6. Woolridge, C. E., Marxman, G. A., and Kier, R. J., Investigation of Combustion Instability in Hybrid Rockets, Stanford Research Institute, NASA CR 66812.

7. Kumar, R. N. and Stickler, D. B., "Polymer Degradation Theory of Pressure Sensitive Hybrid Combustion," Thirteenth Symposium (International) on Combustion. Combustion Institute, Pittsburgh, p. 1059, 1971.

8. United Technology Center, Sunnyvale, California, Solid Fuel Ramjets, Unpublished Report, TM-36-71-U3, 1971.

9. McCarthy, M. J., Pressure Sensitive Combustion in Hybrid Rockets and Solid Fuel Ramjets, Thesis, Naval Postgraduate School, December 1971.

10. Scurlock, A. C., "Flame Stabilization and Propagation in High Velocity Gas Streams," Meteor Report No. 19, Fuels Research Lab., Massachusetts Institute of Technology, May 1948.

11. Longwell, J. P., "Combustion Problems in Ramjets," Fifth Symposium (International) on Combustion, Combustion in Engines and Combustion Kinetics, Reinhold Publishing Corp., New York, p. 48, 1955.

12. Woodward, E. C., "Applications of Chemical Reactor Theory to Combustion Processes," Symposium on the Literature of the Combustion of Petroleum, Advances in Chemistry Series, No. 20, 1956.

13. Avery, W. H., and Hart, R. W., "Combustor Performance with Instantaneous Mixing," Industrial and Engineering Chemistry, Vol. 45, No. 8, p. 1634, August 1953.

14. Gosman, A. D., Pun, W. M., Runchal, A. K., Spalding, D. B., and Wolfshtein, M., Heat and Mass Transfer in Recirculating Flows, Academic Press, 1969.

15. Spalding, D. B., Gosman, A. D., and Pun, W. M., The Prediction of Two-dimensional Flows, Short Course, Pennsylvania State University, August 1972.

16. Spalding, D. B., "A Two Equation Model of Turbulence," Verein Deutscher Ingenieure, Forschungsheft 549, 1972.

17. Holman, J. P., Experimental Methods for Engineers, McGraw-Hill, 1966.

18. Kustov, Y. A. and Rybanin, S. S., "Effect of Chemical Kinetics on the Burning Rate of a Propellant Slab in a Turbulent Oxidizer Flow," Fizika Goreniya i Vzryva, Vol. 6, No. 1, p. 54, 1970.

19. Hojnacki, J. T. and Schwartzkopf, K. G., "Recent Dump Combustor Developments," Ninth JANNAF Combustion Meeting, CPIA Publication No. 231, Vol. II, p. 357, December 1972.

INITIAL DISTRIBUTION LIST

		No. Copies
1.	Defense Documentation Center Cameron Station Alexandria Virginia 22314	2
2.	Library, Code 0212 Naval Postgraduate School Monterey, California 93940	2
3.	Chairman, Department of Aeronautics Naval Postgraduate School Monterey, California 93940	1
4.	Assoc. Professor D.W. Netzer, Code 57Nt Department of Aeronautics Naval Postgraduate School Monterey, California 93940	2
5.	Lt. Lowell D. Boaz, USN Department of Aeronautics Naval Postgraduate School Monterey, California 93940	2
6.	Lt. C. E. Jones III, USN Department of Aeronautics Naval Postgraduate School Monterey, California 93940	1

Security Classification

DOCUMENT CONTROL DATA - R & D

(Security classification of title, body of abstract and indexing annotation must be entered when the overall report is classified)

1. ORIGINATING ACTIVITY (Corporate author)	2a. REPORT SECURITY CLASSIFICATION
Naval Postgraduate School Monterey, California 93940	Unclassified
	2b. GROUP

3. REPORT TITLE

Internal Ballistics of Solid Fuel Ramjets

4. DESCRIPTIVE NOTES (Type of report and, inclusive dates)

Master's Thesis; March 1973

5. AUTHOR(S) (First name, middle initial, last name)

Lowell David Boaz

6. REPORT DATE	7a. TOTAL NO. OF PAGES	7b. NO. OF REFS
March 1973	96	19

8a. CONTRACT OR GRANT NO.	9a. ORIGINATOR'S REPORT NUMBER(S)
b. PROJECT NO.	
c.	9b. OTHER REPORT NO(S) (Any other numbers that may be assigned this report)
d.	

10. DISTRIBUTION STATEMENT

Approved for public release; distribution unlimited.

11. SUPPLEMENTARY NOTES	12. SPONSORING MILITARY ACTIVITY
	Naval Postgraduate School Monterey, California 93940

13. ABSTRACT

An experimental investigation of the internal ballistics of solid fuel ramjets was conducted in order to determine the regression rate of the fuel as a function of chamber pressure, inlet air temperature, and air flux rate, and to model the flow in solid fuel ramjets which use sudden expansion flame-holders at the inlet. In addition, flame stabilization limits were investigated. A computer solution for the non-reacting flow field gave results in good agreement with experiments.

Solid fuel ramjets have an average regression rate of the fuel that closely follows the theoretical expression derived for kinetically controlled hybrid rocket combustion. The inlet step-height-to-motor-diameter ratio is the dominant parameter in determining flame stability limits. However, inlet velocity is also an important parameter.

DD FORM 1 NOV 65 1473 (PAGE 1)

S/N 0101-807-6811

Security Classification

A-31408

14 KEY WORDS	LINK A		LINK B		LINK C	
	ROLE	WT	ROLE	WT	ROLE	WT
Ramjet Solid Fuel Recirculating Flow Internal Ballistics